Review

Bacterial peroxidases – Multivalent enzymes that enable the use of hydrogen peroxide for microaerobic and anaerobic proliferation ☆

Daniela S. Barreiro [a,b], Ricardo N.S. Oliveira [a,b], Sofia R. Pauleta [a,b,*]

[a] *Microbial Stress Lab, UCIBIO, Departamento de Química, FCT-UNL, Associate Laboratory i4HB, Institute for Health and Bioeconomy, NOVA School of Science and Technology, Universidade NOVA de Lisboa, 2829-516 Caparica, Portugal*
[b] *Microbial Stress Lab, UCIBIO – Applied Molecular Biosciences Unit, Department of Chemistry, NOVA School of Science and Technology, Universidade NOVA de Lisboa, 2829-516 Caparica, Portugal*

ABSTRACT

Bacterial peroxidases are responsible for the reduction of hydrogen peroxide to water. Found in the periplasm of gram-negative bacteria, they are one of the defense mechanisms against endogenous and exogenous peroxide stress under low oxygen tensions. Besides being involved in peroxide detoxification, bacterial peroxidases have been proposed to constitute an alternative pathway to the respiratory chain under anoxic conditions, as demonstrated in *E. coli* that can use hydrogen peroxide as an electron acceptor in the absence of oxygen.

Bacterial peroxidases are *c*-type cytochromes with either two or three *c*-type hemes bound to the polypeptide chain, being divided into classical or non-classical, respectively. Orthologous to the classical bacterial peroxidases are the MauG enzymes that share some structural, spectroscopic and sequence similarities but have distinct physiological roles (though for most their function remains unknown).

The spectroscopic and kinetic data on bacterial peroxidases are reviewed for both classes. Most classical bacterial peroxidases require reductive activation that consists in structural changes so that the catalytic heme becomes accessible to the substrate. However, non-classical enzymes are ready to bind the hydrogen peroxide as their catalytic center is penta-coordinated, which is also observed in their structural model. The few studies that report the involvement of bacterial peroxidases from pathogenic bacteria in biofilms, is an indication that these enzymes might contribute to their infection mechanism and thus can constitute alternative drug targets.

Contents

1. Introduction

Metals ions are involved in several biological processes as cofactors of proteins. Their ability to alternate between oxidation states allows the catalysis of oxidation–reduction reactions, which are the basis of many cellular processes. From ancient times, Nature has evolved and developed strategies to overcome metal availability and its solubility. Consequently, there are enzymes with similar metal cofactors that catalyze different reactions, and enzymes catalyzing the same reaction but harboring different metal cofactors. One of the later cases are peroxidases, which catalyze the two-electron reduction of hydrogen peroxide to water (Eq. (1)), using a variety of oxidizable substrates, such as aromatic molecules, halides, cations (e.g., Mn^{2+}) and small electron transfer proteins.

$$H_2O_2 + 2\ e^- + 2\ H^+ \rightarrow 2\ H_2O\ E\circ = 1.76\ V,\ \Delta G = -339.7\ kJ/mol$$

(1)
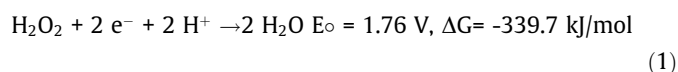
Although this reaction can be catalyzed by metal-dependent and metal-independent enzymes [1–3], in here we will only focus on the former. A brief overview of the metal-dependent peroxidases will be given in this introduction, focusing primarily on their coordination spheres. These enzymes are the vanadium-dependent
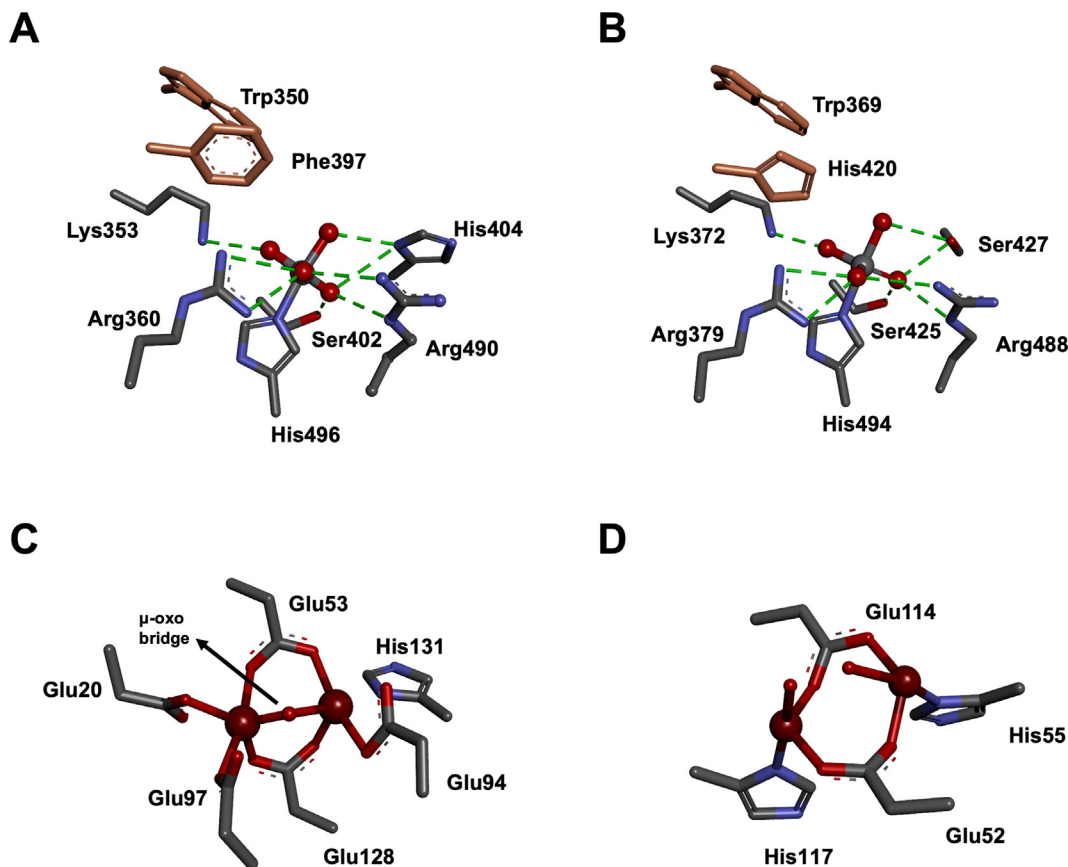
Fig. 1. The catalytic center of vanadium-dependent haloperoxidases and di-iron peroxidases. The coordination of vanadate in chloroperoxidase from *C. inaequalis* and *Streptomyces* sp. CNQ-525 is shown in Panel A and B, respectively. The core residues coordinating the vanadate are colored by element, and the H-bonds are represented as green dashed lines, and the residues in the second coordination sphere are in orange. The coordination of the di-iron center in rubrerythrin from *D. vulgaris* Hildenborough and from *P. furiosus* are shown in Panel C and D, respectively. The coordinating residues are colored by element. Figures were prepared with Discovery Studio Visualizer using the coordinates PDB ID 1IDQ (A), 3W36 (B), 1RYT (C) and 3PWF (D).

haloperoxidases, the di-iron peroxidases and heme-peroxidases. The focus of this review is the bacterial peroxidases, which although being heme-dependent peroxidases, harbor in their catalytic center a *c*-type heme instead of the *b*-type heme found in the superfamily of heme-dependent peroxidases and are only found in bacteria. For this reason, these were considered to be a different superfamily of peroxidases.

1.1. Vanadium-dependent haloperoxidases

Vanadium-dependent haloperoxidases are enzymes that use H_2O_2 to oxidize a halide ion that becomes a strong reactive electrophilic intermediate able to halogenate certain organic substrates. This process increases the reactivity of halogenated natural organic compounds and/or its antifungal, antibacterial and antiviral properties. Depending on the type of halide, chloride, bromide, or iodide, used as co-substrate, these enzymes are classified as chloroperoxidases, bromoperoxidases or iodoperoxidases, respectively.

Vanadium-dependent haloperoxidases have been isolated from bacteria, fungi, and algae [4]. The vanadium ion is present in the enzyme as vanadate (VO_4^{3-}) coordinated by one histidine and four oxygen atoms in a pentacoordinated trigonal bipyramidal geometry (Fig. 1A and B). Overall, vanadium-dependent haloperoxidases have their cofactor in this geometry, however some differences have been observed: (i) *Streptomyces* sp. CNQ-525 vanadium-dependent chloroperoxidase has similar length V-O bonds, though longer than the ones observed in the vanadium cofactor of chloroperoxidase from the fungus *Curvularia inaequalis*; (ii) in the *Ascophyllum nodosum* vanadium-dependent bromoperoxidase the coordination geometry of the vanadium is similar to the one in the *C. inaequalis* chloroperoxidase but slightly distorted due to the shorter length of one of its V-O bond; (iii) in the *Zobellia galactanivorans* vanadium-dependent iodoperoxidase, its cofactor has a tetrahedral geometry with V-O bonds longer than those in the catalytic center of *C. inaequalis* chloroperoxidase and *A. nodosum*

bromoperoxidase [5]. Regarding the second coordination sphere, there are five core residues H-bonding the oxygen atoms coordinating the vanadium (Lys, Ser, His and two Arg), and other two residues in the vicinity of the center (Trp and Phe) (Fig. 1A). In *Streptomyces* sp. chloroperoxidase, the core histidine residue is replaced by a second serine and the phenylalanine is replaced by a histidine (Fig. 1B). In the A. *nodosum* bromoperoxidase this phenylalanine is replaced by a histidine but the other core residues are the same as the ones found in *C. inaequalis* chloroperoxidase [6].

1.2. Di-iron peroxidases – Rubrerythrin

Rubrerythrin is an enzyme present in anaerobic/microaerophilic bacteria and archaea involved in the defense mechanisms against oxidative stress by reducing H_2O_2 to water [7]. Rubrerythrin is a non-heme peroxidase with two metal cofactors: a rubredoxin-like iron center [Fe(Cyst)$_4$] and a di-iron center [8]. The two most studied enzymes have been isolated from the anaerobic bacterium *Desulfovibrio vulgaris* [9] and anaerobic archaeon *Pyrococcus furiosus* [10]. In the structure of the *D. vulgaris* rubrerythrin, the two iron ions are bridged by a μ-oxo-bond, and each iron atom is coordinated by three residues, one iron by three glutamates and the other by two glutamates and one histidine sidechain (Fig. 1C) [11]. In the *P. furiosus* rubrerythrin, the two irons are each coordinated by two glutamates and one histidine sidechain (Fig. 1D) [12].

1.3. Heme peroxidases

Most peroxidases are heme-dependent peroxidases, having in their active center a *c*- or a *b*-type heme or post-translationally modified versions of the later, and differing also in the axial coordination of the heme–iron. Whereas the *c*-type heme dependent peroxidases are only identified in bacteria (the main focus of this review), the other heme-dependent peroxidases have been found
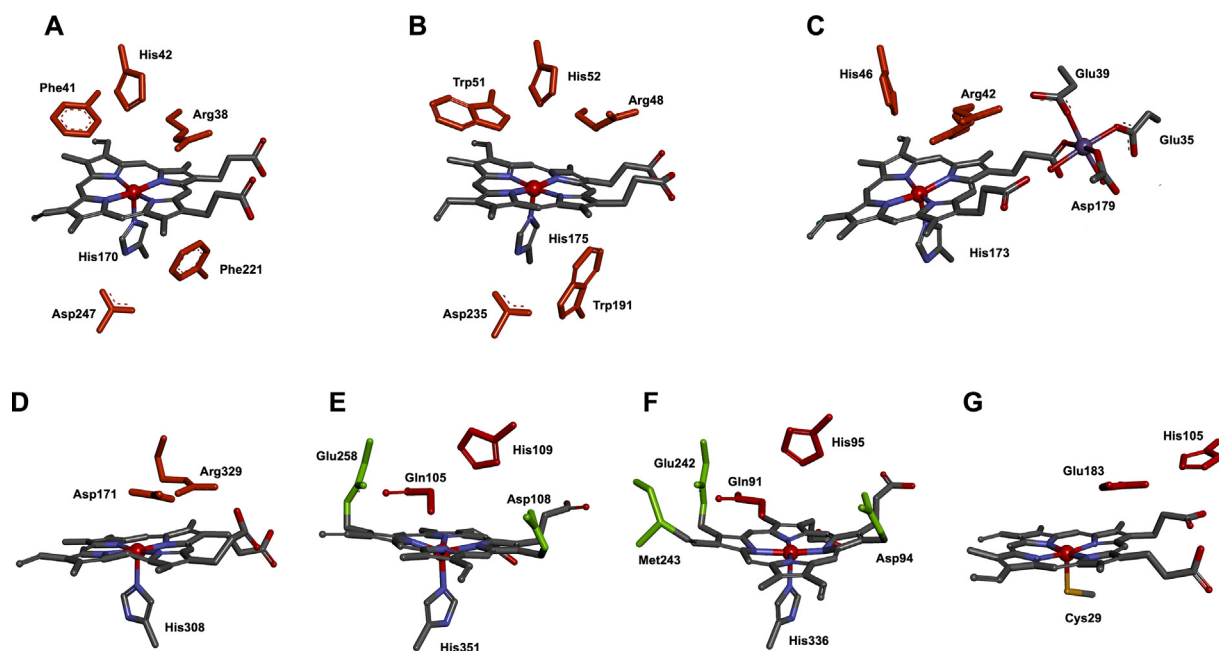
Fig. 2. Catalytic center of heme-dependent peroxidases with a *b*-type heme in the catalytic center. (A) Horseradish, (B) *S. cerevisiae* cytochrome *c* peroxidase, (C) Mn-dependent peroxidase, (D) DyP-type peroxidase, (E) lactoperoxidase, and (F) human myeloperoxidase, and (G) chloroperoxidase from *Leptoxyphium fumago*. The heme group and iron coordinating residues are colored by element, residues involved in covalent bonds between the heme and the polypeptide chain are in green, and residues from the second coordination sphere are in red. Figures were prepared with Discovery Studio Visualizer using the coordinates PDB ID 1H5A (A), 2CYP (B), 3M5Q (C), 2D3Q (D), 3GC1 (E), 5FIW (F), and 1CPO (G).

in all kingdoms of life and phylogenetically have been divided into four superfamilies: (i) peroxidase–catalase, (ii) peroxidase–cyclooxygenase, (iii) peroxidase–chlorite dismutase and (iv) peroxidase–peroxygenase [13–16]. This classification should start to be widely adopted in the literature for clarity, as already proposed [13–16].

The first two peroxidases to be isolated 60 decades ago were the horseradish peroxidase from *Armoracia rusticana* [17,18] and the mitochondrial cytochrome *c* peroxidase from *Saccharomyces cerevisiae* [19], that belong to large peroxidase–catalase superfamily. These enzymes bind a single *b*-type heme as a catalytic center, with the heme iron being penta-coordinated with a histidine residue in the axial proximal position (His175 in *S. cerevisiae* cytochrome *c* peroxidase) [20]. In the second coordination sphere of the heme there are two well-conserved residues, an arginine and a histidine (Arg48 and His52 in *S. cerevisiae* cytochrome *c* peroxidase) (Fig. 2A and B). In *S. cerevisiae* cytochrome *c* peroxidase, there are also two tryptophane residues, Trp51 and Trp191, with the second making Van der Waals interaction with the axial histidine ligand and the porphyrin ring and being involved in the formation of an intermediate of the catalytic cycle (Compound I, Trp radical). In addition, there is also an aspartate (Asp235 in *S. cerevisiae* cytochrome *c* peroxidase) H-bonding the axial histidine and tryptophan residues [20,21] (Fig. 2B). These two enzymes are the two most extensively studied peroxidases, and their catalytic mechanism is well characterized [21,22] and it has served as a starting point for understanding the mechanism of other heme peroxidases [21].

Manganese peroxidases are extracellular heme-containing peroxidases found in white-rot fungi and some bacteria, that also belong to the peroxidase-catalase superfamily. In these enzymes the manganese ion (Mn^{2+}) acts as the electron donor, while also being able to oxidize a wide range of substrates [23]. Manganese peroxidases are glycoproteins with a globular structure composed mostly of α-helices and harboring multiple disulfide bridges. The heme cofactor in this enzyme is penta-coordinated with one histidine residue (His173 in the manganese peroxidase from *Phanerochaete chrysosporium*), similar to the catalytic center of cytochrome *c* peroxidase. The second coordination sphere is well-conserved among these enzymes and comprise a histidine and an arginine residue (His46 and Arg42 in the manganese peroxidase from *P. chrysosporium*) (Fig. 2C). The Mn ion is coordinated by two glutamate residues and one aspartate (Glu35, Glu39 and Asp179 in the manganese peroxidase from *P. chrysosporium*), as well as a propionate group from the heme and two water molecules [24], displaying an octahedral geometry. The two metal ions present in manganese peroxidase undergo redox changes during the catalytic cycle [23,25,26]. The hydrogen peroxide binds to the ferric form (Fe^{3+}), initiating the catalytic cycle, and one H_2O molecule is released leading to the formation of an Fe^{4+}-oxo porphyrin radical (Compound I). The Mn^{2+} will then function as an electron donor to this radical, being oxidized to Mn^{3+}, with formation of Compound II. Then, again Mn^{2+} is oxidized to Mn^{3+}, releasing a second H_2O molecule, and the heme iron returns to the initial ferric state. During this cycle, Mn^{3+} is able to oxidize different substrates [25].

The dye-decolorizing peroxidases (DyP-type peroxidases) belong to the peroxidase–chlorite dismutase superfamily. Similarly to the manganese peroxidases and other peroxidases [27], DyP-type peroxidases can efficiently degrade lignin-derived compounds, anthraquinones and azo dyes [28,29]. These enzymes are found in basidiomycetes, bacteria, and fungi, and differ from other heme-dependent peroxidases in structure and have different catalytic properties. They are versatile enzymes that can exhibit, besides the usual reactivity towards peroxides, also hydrolase and oxidase activity. DyP-type peroxidases have been found distributed over different cell compartments, such as the periplasm,

within encapsulin (when these function as cargo proteins) and can even be secreted as extracellular enzymes [28].

The DyP-type peroxidases are mono-hemic enzymes, with one heme group penta-coordinated by a histidine (His308 in the DyP-type peroxidase from *Bjerkandera adusta*) [30]. The general motif GXXDG, a well-conserved region of DyP-type peroxidases, has a conserved aspartate (Asp 171 in the DyP-type peroxidase from *B. adusta*) that substitutes the conserved histidine in other peroxidases, leading to a lower optimal pH. The conserved Arg329, together with Asp171, form the second coordination sphere of the heme in the DyP-type peroxidase from *B. adusta* (Fig. 2D).

Examples of the peroxidase–cyclooxygenase superfamily are the mammalian haloperoxidases, which are homologous in function to vanadium-dependent haloperoxidases [13]. Crystal structures of lactoperoxidase [31–33] and myeloperoxidase [34,35] showed the presence of a modified protoporphyrin IX covalently bound to the polypeptide chain through two ester bonds between the pyrrole methyl groups and one glutamate and one aspartate residues (Fig. 2E and F), and in myeloperoxidase there is an additional bond between one pyrrole vinyl group and a methionine forming a sulfonium ion bond (Fig. 2F). Due to these post-translational modifications the heme has a particular distortion, which contributes to their distinctive redox and spectroscopic properties.

The chloroperoxidase from the fungus *Leptoxyphium fumago* and the bromoperoxidase from the plant *Agrocybe aegerita* belong to the peroxidase–peroxygenase superfamily. These peroxidases have a penta-coordinated *b*-type heme with a cysteine as the distal ligand coordinating the heme iron through a thiolate bond (Fig. 2G) and catalyze the incorporation of peroxide-derived oxygen into the substrate. Due to this unusual coordination for a peroxidase, these enzymes are also known as heme-thiolate haloperoxidases [36].

2. Bacterial peroxidases superfamily

Bacterial peroxidases are periplasmatic enzymes that have two (or three) *c*-type hemes as cofactors, each in a structural domain. In addition, they can receive electrons from type-I copper proteins, *c*-type cytochromes or from the quinol pool, and thus a designation of 'Bacterial peroxidases', should be adopted, in detriment of the designation of "bacterial cytochrome *c* peroxidase" that is still found in the literature.

Bacterial peroxidases are the main subject of this review, that specifically will be centered on their phylogenetic organization, physiological role, biochemical properties and the currently accepted catalytic mechanism, as will be discussed in the following sections.

2.1. Phylogenetic distribution

Bacterial peroxidases belong to the CCP_MauG superfamily (cytochrome *c* peroxidase_MauG PF03150) that comprises di-heme enzymes able to reduce hydrogen peroxide to water. A phylogenetic relationship based on the primary sequence of these enzymes is presented in Fig. 3. There is a clear division between two groups: (i) the bacterial peroxidases (pink square) and (ii) MauG orthologs (blue square). Both groups can be further divided into two families. The bacterial peroxidases are divided into classical and non-classical, with the first comprising the di-hemic enzymes and the second the tri-hemic enzymes, while the MauG related enzymes can also be divided into two groups: MauG, encoded by the *mau* operon, and related enzymes but encoded in other operons, though their phylogenetic organization does not seem to be so clear (Fig. 3).
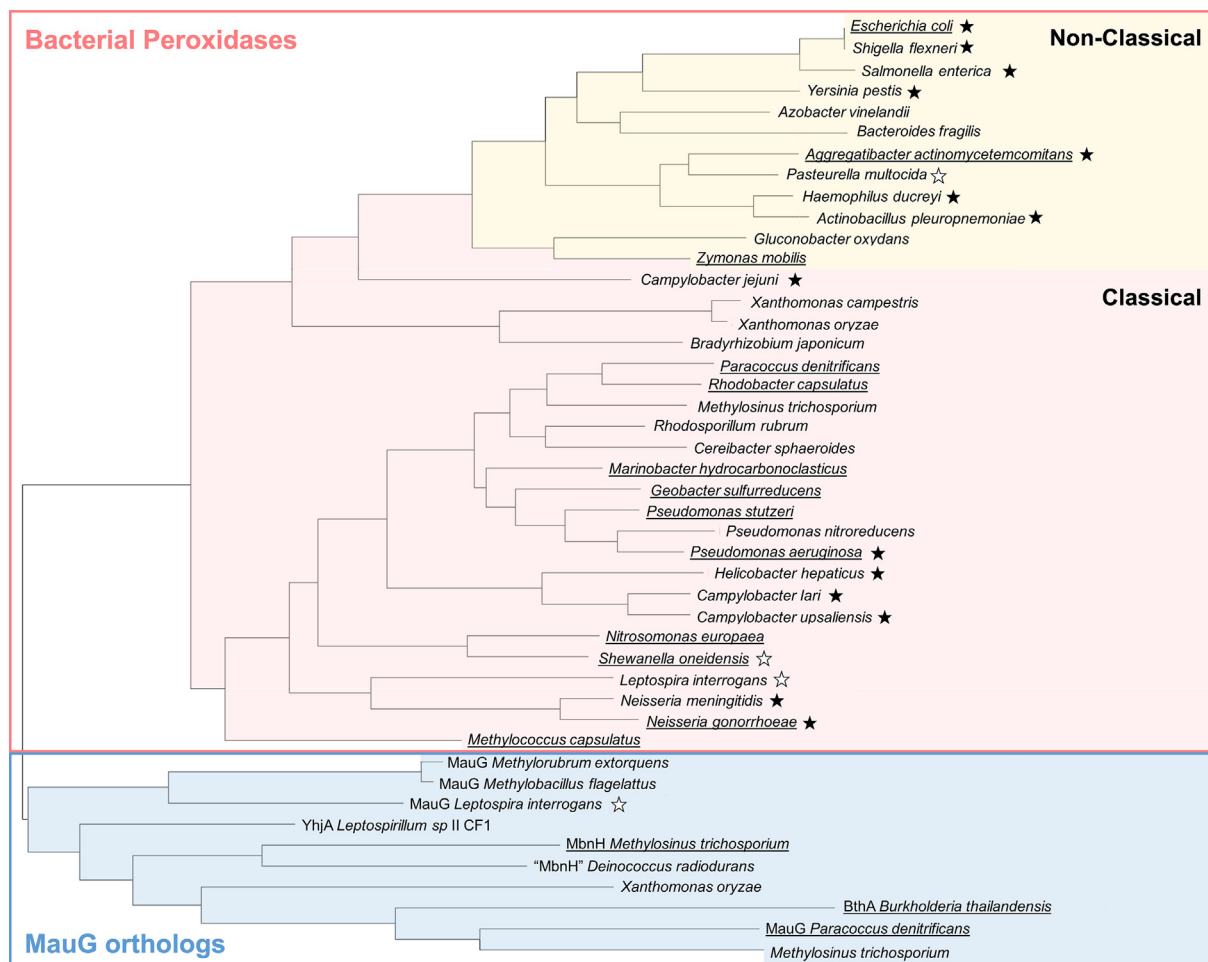
Fig. 3. Phylogenetic tree of CCP_MauG proteins. Bacterial peroxidases are present within the pink square: classical within pink area and non-classical bacterial peroxidases within the yellow area. The 'MauG ortologs'are within the blue area (proteins identified as MauG are encoded by the *mau* operon and the others are annotated as CCP_MauG but have unknown function). White and black stars identifies zoonotic and human pathogens, respectively, isolated enzymes are underlined. Maximum-Likehood phylogeny method bootstrap statistical analysis with Molecular Evolutionary Genetics Analysis [37].

The MauG orthologous enzymes share some features with classical bacterial peroxidases, namely the overall three-dimensional structure and the presence of two *c*-type hemes bound to the polypeptide chain, in distinct domains (Fig. 4). They also have a tryptophan residue and a calcium ion between the two hemes, required for the intramolecular electron transfer, and regulation of the heme coordination and their reduction potential (*vide infra*). In these enzymes, the catalytic heme (peroxidatic heme, P Heme) is penta-coordinated or binding a H_2O/OH^- molecule in the active state. However, they differ in the coordination of the heme that receives the electrons required for catalysis (electron transferring heme, E Heme), that is Met/His hexacoordinated in bacterial peroxidases (Fig. 4A), while in MauG orthologous enzymes, this heme is Tyr/His hexacoordinated (Fig. 4B and 4C).

One of the best characterized MauG enzymes is the one from *Paracoccus denitrificans*, which is encoded in *mauG* from the *mau* operon. These enzymes are involved in the synthesis of tryptophan-typrophanphylquinine, the cofactor of methylamine dehydrogenase (Fig. 4B) [38–40]. The other group of MauG orthologs harbour enzymes closely related to MauG in terms of their spectroscopic features and peroxidatic activity but their encoding gene is not part of the *mau* operon. This is a heterogeneous group with the enzymes being involved in very distinct functions and encoded in genes with non-related gene organization. So far three of these enzymes have been isolated and characterized,

Methylosinus trichosporium MbnH [41,42], *Burkholderia* sp BthA [43–45], and *Leptospirillum* sp. CF-1 YhjA [46].

MbnH homologues are encoded in the genome of most methanotrophic bacteria, such as *M. trichosporium*, in an operon harboring another gene coding for MbnP. These bacteria have a high demand of copper for the biosynthesis of methane monooxygenase, and these two proteins are proposed to be involved in copper homeostasis, with MbnP being a copper binding protein, while MbnH specific role is unclear as its natural substrate is not yet known [41,42].

Leptospirillum sp. CF-1, an iron-oxidizing acidophilic bacterium [47], encodes YhjA in an operon between *perR*, encoding a global peroxide-responsive transcription factor, and *ahpC*, encoding an alkyl hydroperoxide reductase [46]. The YhjA enzyme has been identified as a bacterial peroxidase but similarly to the other MauG orthologous, the methionine residue that coordinates the E heme is substituted by a tyrosine and thus it is not a true bacterial peroxidase. Nevertheless, this enzyme is proposed to have an important role in hydrogen peroxide reduction required in the first stages of biofilm formation over mineral substrates [46].

Deinococcus radiodurans genome has two genes annotated as bacterial peroxidases [48]. However, a closer inspection of the primary sequence revealed that one (DR_A0145) has homology to dye-decolorizing peroxidases [49] and the other has the conserved tyrosine residue as E heme distal axial ligand and should be
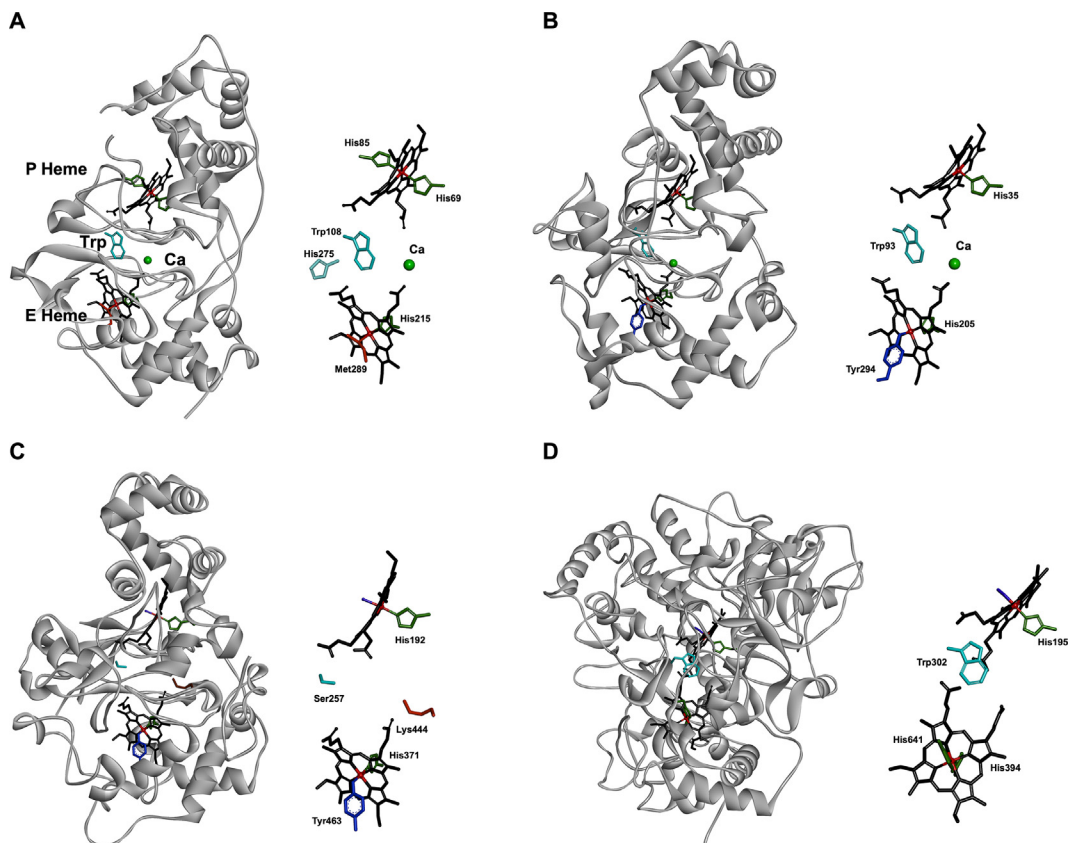
Fig. 4. Structural representation of CCP_MauG superfamily orthologs and their heme coordination: (**A**) *Paracoccus pantotrophus* bacterial peroxidase in the oxidized form, (**B**) MauG from *Paracoccus denitrificans*, (**C**) BthA from *Burkholderia thailandensis*, and (**D**) RoxA from *Xanthomonas* sp. 35Y. The backbone is represented by the secondary structure with the two hemes in similar orientation, hemes are represented as sticks in black with the iron atom in red, and its coordinating residues colored by atom type, the tryptophan or serine (in **C**) bridging the two hemes is shown as cyan stick, and the calcium ion is represented as a green sphere. Only the monomer is shown for simplicity. Figures were prepared in Discovery Studio Visualizer using coordinates PDB ID 2C1U (A), 3L4M (B), 6NX0 (C) and 4B2N (D).
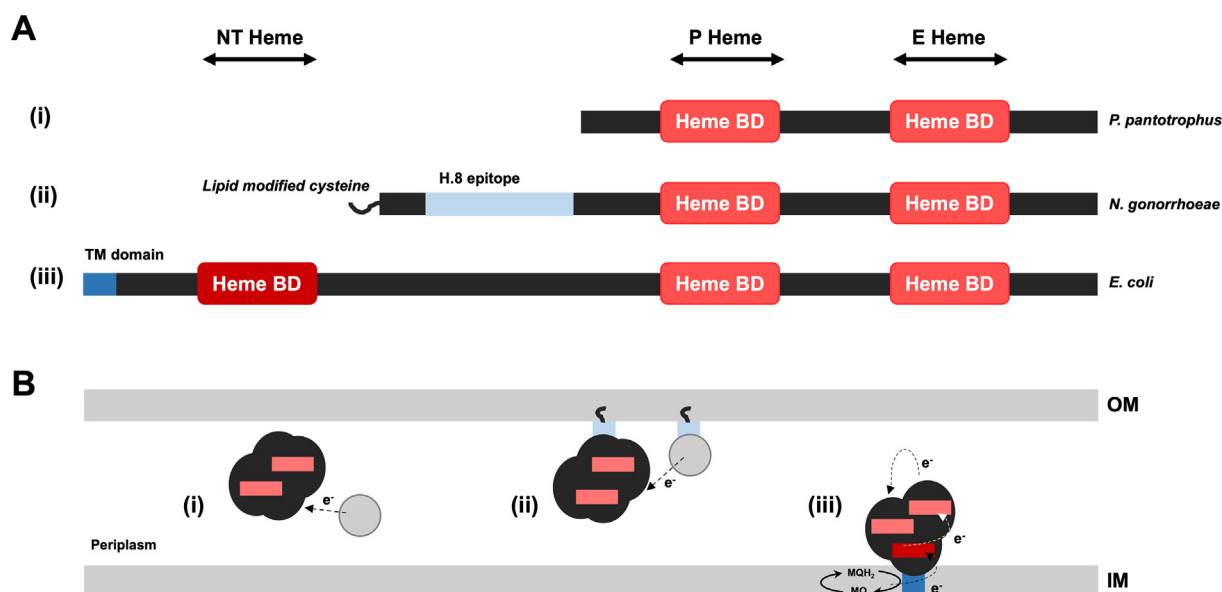
Fig. 5. Schematic representation of classical and non-classical bacterial peroxidases primary sequence organization and cellular localization. (**A**) Representation of primary sequence of bacterial peroxidases with the identification of the heme binding domains (BD) of different *ccp* genes identified so far (**i**) *Paracoccus pantotrophus* has a soluble bacterial peroxidase with two *c*-type heme binding domains. (**ii**) *Neisseria gonorrhoeae* has an outer membrane bound bacterial peroxidase through a lipid modified cysteine with two *c*-type heme binding domains. (**iii**) *Escherichia coli* has an inner membrane bound bacterial peroxidase through a transmembrane helix with three *c*-type heme binding domains. (**B**) Representation of their cellular localization in the periplasm. The grey circles represent the electron donor proteins.

grouped in this MauG ortholog family. Similarly, in the genome of *Flavobacterium psychrophilum*, an aquaculture pathogen responsible for the bacterial cold-water disease in fish, the gene annotated as *ccp* gene [50] should be named as CCP_MauG (though the primary sequence shares 32% identity with bacterial peroxidases, the distal ligand of E heme seems to be a tyrosine). Transcriptomic analysis of biofilms showed that this gene was upregulated with a 5-fold increase in comparison to planktonic cells [51].

The gene coding for BthA from *Burkholderia thailandensis*, *bthA*, is located downstream of a putative phosphatase gene, but although it has peroxidatic activity its physiological role has not yet been identified. This enzyme is able to stabilize a bis-Fe^{4+} species, similar to the one observed in MauG [43,44], but has distinct features from bacterial peroxidases and MauG enzymes, including a different mechanism for hydrogen peroxide reduction than the one of bacterial peroxidases [43,45]. The conserved tryptophan located between the two hemes is substituted by a serine and the calcium ion is absent, but there is a lysine residue (Lys444) proposed to be responsible for maintaining the water network in between the proprionates of the two heme cofactors that will assist in the intramolecular electron transfer (Fig. 4C) [43,45].

RoxA from *Xanthomonas* sp., encoded by *roxA*, is an oxygenase that catalyzes the conversion of *cis*-1,4-polyisoprene, present in the latex milk from rubber trees to 12-oxo-4,8-dimethyl-tri deca-4,8-diene-1-al [52,53]. The similarities with CCP_MauG lies only on the core structure of its heme domains, as it presents low sequence homology with mainly unordered (loops) structure responsible for its higher molecular weight (75 kDa) (Fig. 4D) [54]. Structural similarities include the hemes orientation with the conserved tryptophan in between them, the coordination of P heme, though E heme is bis-His hexacoordinated [54] (Fig. 4). Thus, suggesting that RoxA and CCP_MauG are evolutionary related enzymes (Fig. 4).

The analysis of the phylogenetic tree indicated that bacterial peroxidases are divided into classical and non-classical bacterial peroxidases, depending on the number of *c*-type hemes and their cellular localization. Classical bacterial peroxidases are homodimers binding two *c*-type hemes (Fig. 4A), one in each globular domain of the polypeptide chain, either anchored to the outer-membrane or soluble in the periplasm (Fig. 5). Classical bacterial peroxidases have been isolated and characterized from several organisms, and their biochemical properties will be discussed in Section 3. Non-classical bacterial peroxidases bind three *c*-type hemes and are anchored to the inner-membrane through a transmembrane helix (Fig. 5 and Fig. 9). The two hemes located in the C-terminus domain are homologous to the two hemes from classical bacterial peroxidases, whereas the third heme is located in the N-terminus, comprising a completely new additional domain [55] (Fig. 5 and Fig. 9), as will be discussed in Section 4. Significant research on non-classical bacterial peroxidases has only started in the last decade and so far, these enzymes have been isolated from *Aggregatibacter actinomycetemcomitans* [55–58], *Zymomonas mobilis* [59] and *Escherichia coli* [60]. *Salmonella typhimurium* and *Yersinia pestis* are pathogenic agents harboring in their genome a gene encoding a tri-hemic bacterial peroxidase, but their isolation has not yet been reported (Fig. 3).

2.2. Gene regulation and expression

Bacterial peroxidases encoding gene, *ccp*, has been found in several Gram-negative bacteria, including pathogens, such as *Neisseria*, *Salmonella*, *Aggregatibacter* and *Yersinia* genus, but it is absent in Gram-positive bacteria and archaea. Mainly present in the genome as a single copy, some species harbor more than one *ccp* homologous gene, as is the case of *Geobacter*

Table 1
Summary of the spectroscopic properties of classical bacterial peroxidases studied up to date.

Organism	As-isolated (Oxidized)					Mixed-Valence State						Refs
	E heme		P heme			E heme	P heme					
	1H-NMR (ppm)	EPR (gmax)	1H-NMR (ppm)	EPR (gmax)	Soret / HS bands[a] (nm)	Soret band (nm)	Soret band (nm)	1H-NMR (ppm)	EPR (gmax)	Soret / HS bands[a] (nm) Without added Ca^{2+}	Addition of Ca^{2+}	
CcpA *Geobacter sulfurreducens*	-	-	-	-	407 / 620	407	417	-	-	407 / 620	No effect	[111]
MacA *Geobacter sulfurreducens*	-	-	-	-	407 / 620	407	419	-	-	407 / 620	-	[61]
Marinobacter hydrocarbonoclasticus 617	-	-	-	-	407 / 640	407	418	-	-	406	397/640	[68]
Methylococcus capsulatus	-	3.23 / 6.28	-	2.79	409 / 360, 630	406	419	-	2.79	407 / 625	-	[107]
Neisseria gonorrhoeae	-	3.18 / 6.28	-	2.99	402 / 360, 620	402	418	-	2.88	402 / 620	No effect	[110]
Nitrosomonas europaea	-	3.37	-	2.81	408 / 630	408	418	-	2.89	408 / 630	-	[106,126]
Paracoccus pantotrophus	58.2, 55.0 51.5	3.41 / 6.0	33.2, 23.8	3.0	409 / 380, 640	409	418	64.0, 57.0, 55.5, 51.0	2.89[b]	409 / 380, 640	397/640	[113,122]
Pseudomonas aeruginosa	45-65	3.3 / 5.8	21.5, 19.5	3.0	407 / 630	407	418	45-65	2.85	408 / 630	-	[119,121,136]
Pseudomonas stutzeri	69.3, 64.1 57.3, 55.9	3.39 / 5.7	32.0, 22.7	3.0	408 / 380, 630	408	418	62.0, 55.9, 55.1, 53.5	2.92	408 / 380, 630	No effect	[108,109]
Rhodobacter capsulatus	-	-	-	-	406 / 630	406	418	-	-	406 / 630	No effect	[128]
Shewanella oneidensis	-	3.40	-	3.1	407	407	417	-	2.87	407 / 640	-	[112,126]

[a] HS - High-spin.
[b] The signal with a g_{max} at 2.89 is observed in the presence of excess calcium.

sulfurreducens [61] and *Campylobacter jejuni* [62], though the reasons for this are not yet clear. In some organisms, the gene is named *yhjA* as is the case of *E. coli* [63].

The expression of *ccp* gene and its regulation have only been studied for a few species, which identified two transcriptional regulators: OxyR, a transcription factor that responds directly to H_2O_2, and FNR (fumarate and nitrate reduction regulatory protein), an oxygen-responsive global transcription factor. These regulators can either control the expression of *ccp* independently or together, as it is the case of *ccp* from *Bacteroides fragilis* (gene encoding a tri-hemic bacterial peroxidase under the control of OxyR) [64], *Neisseria gonorrhoeae* and *P. denitrificans* (under the control of FNR) [65,66], and *yhjA* from *E. coli* (co-regulated by OxyR and FNR) [63].

The regulation of *ccp* by FNR has been demonstrated by analyzing the *ccp* expression and enzyme levels when the microorganism was grown under different conditions. In *Paracoccus pantotrophus* and *Marinobacter hydrocarbonoclasticus* 617 high aeration rates of the culture medium were shown to result in low yields of bacterial peroxidase [67,68]. More thorough studies in *P. denitrificans* reported that a *fnr* knockout strain grown under microaerophilic conditions and an aerobically grown wild-type strain lacked this enzyme, whereas a microaerophilic grown wild-type showed the presence of bacterial peroxidase [66]. In *N. gonorrhoeae*, *ccp* was reported to be expressed mainly under anaerobic conditions, being repressed in the presence of oxygen [65]. In the case of *Shewanella oneidensis*, CcpA, the bacterial peroxidase from this organism is also shown to be produced under anaerobic conditions, and its presence seems to be a metabolic advantage during dissimilatory iron-reducing conditions [69].

Hydrogen peroxide is a product of superoxide dismutation. As a ROS itself, superoxide is generated under anoxic conditions, presuming an impairment in the electron flow in the respiratory pathway [3,70]. This results in increased levels of the semiquinone Q that reduces O_2 to H_2O_2 [71,72]. Additionally, FNR is a protein with two iron-sulfur clusters responsible for the assemble of the DNA-binding state of the regulator. Due to the high sensitivity of the iron-sulfur clusters, that disassemble in the presence of O_2, FNR is only active under anaerobic conditions [73,74]. Therefore, this is consistent with *ccp* expression under anaerobic conditions, in which H_2O_2 production is promoted (*vide infra*).

2.3. Physiological role of bacterial peroxidases

Several physiological roles have been attributed to bacterial peroxidases with the main *in vivo* function being the detoxification of exogenously- or endogenously-produced H_2O_2 [3,75], which enables these enzymes to take part in different metabolic pathways that can be related with ROS detoxification, metal reduction metabolism or the use of hydrogen peroxide as electron acceptor.

The obligate human pathogen *N. gonorrhoeae*, responsible for the sexually transmitted disease gonorrhea, has a higher susceptibility to H_2O_2 when *ccp* and the gene encoding a cytoplasmatic catalase (*katA*) are mutated, when compared to the single *katA* mutant [76]. In *A. actinomycetemcomitans*, another human pathogen, a *ccp* null mutant showed an increase in sensitivity to endogenous peroxide stress, as well as the absence of a secreted leukotoxin, LtxA [56], which is degraded in the presence of ROS [77]. LtxA is responsible for the membrane disruption of leukocytes and erythrocytes, thus considered the major virulence agent of *A. actinomycetemcomitans* [78–80]. Additionally, in *C. jejuni*, deletion of the two putative *ccp* genes resulted in a 50-fold decrease of its commensal colonization ability [81]. This suggests that these proteins play a role in bacterial colonization, coupled to pathogenic virulence, in response to oxidative stress produced by the host immune system or by the microbiota of the infection site, to prevent bacterial proliferation.

In *G. sulfurreducens*, MacA, one of the putative bacterial peroxidases isolated from this microorganism, receives electrons from PpcA [61,82], and it is reported to detoxify hydrogen peroxide generated as a by-product of Fe^{3+} reduction [83,84], and possibly other metals, as U^{6+} [85], but not to respond to oxidative stress [86]. The other bacterial peroxidase from the same organism, CcpA, was shown to be associated with the use of Fe^{3+} and Mn^{4+} [83]. A similar function to MacA has been attributed to CcpA from *S. oneidensis* that is proposed to receive electrons from the cytochrome ScyA during Fe^{3+}-oxidizing conditions [69].

Bacterial peroxidase enables the cells to utilize hydrogen peroxide as a terminal electron acceptor, supporting respiration under anoxic conditions. For that a proton motive force necessary for ATP synthesis must be established across the inner membrane, through the involvement of primary dehydrogenases and/or by the bc_1-type cytochrome complex that then reduce electron carriers, either small shuttle proteins or menaquinol, that donate electrons to bacterial peroxidases.

The contribution of classical bacterial peroxidases to the respiratory chain has been proposed in catalase-negative *Campylobacter mucosalis* grown in formate, that established a 0.6 H^{1+}/H_2O_2 pumping stoichiometry [87]. In the case of non-classical bacterial peroxidases, YhjA from *E. coli* has been demonstrated to be required to maintain respiration under anoxic conditions by reducing hydrogen peroxide to water and receiving electrons from menaquinol [60].

Thus, bacterial peroxidases seem to play a crucial role in pathogenic and non-pathogenic bacteria by enabling them to thrive in anoxic environments with high concentrations of H_2O_2. In fact, these conditions are met either as a byproduct of dissimilatory metal reduction, but also inside phagosomes, in the presence of lactic acid bacteria, or in oxic-anoxic interfaces that can occur in biofilms, or for instance in the gut where sulfate reducing bacteria can induce formation of H_2O_2, through the production of sulfides [88].

2.3.1. Contribution to biofilm

Bacterial biofilms communities are an emergent health concern as they have been associated with the increase of bacterial pathogenesis. In fact, being clusters of bacteria embedded in a self-produced extracellular matrix, biofilms' main goal is to protect the bacteria from damage in a hostile environment. Biofilms are very heterogenous and complex structures that can harbor several types of bacteria with the ability to have pH-, nutrient- and/or O_2-gradients through its different layers [89,90].

Bacterial peroxidase encoding gene and its transcription regulators can potentially be upregulated in a biofilm community, in response to low oxygen tensions and elevated levels of H_2O_2. In the literature, the only reports of the involvement of bacterial peroxidases in biofilms come from studies on pathogenic bacteria (*vide infra*) evidencing that these enzymes can be an important trait under such conditions.

One case is *N. gonorrhoeae*, which was shown to be able to form biofilms over glass surfaces, as well as on primary urethral epithelial cells and cervical cells [91]. The *ccp* gene in this organism is regulated by FNR, but, contrary to OxyR [92], no studies have been reported on the effect of that transcription regulator on biofilm formation. Nonetheless, transcriptomic profiling of *N. gonorrhoeae* biofilms demonstrated that *ccp* is upregulated > 2.5-fold in biofilms formed over a glass when compared to planktonic cells [93] and its mRNA was also reported to have a 4–6-fold increase in human cervical epithelial cells [93]. These findings were further corroborated by proteomic studies, that showed a > 2-fold increase in the bacterial peroxidase present in biofilm compared to planktonic cells [94].

The high level of airway mucus-infections by *Pseudomonas aeruginosa* in cystic fibrosis patients has been attributed to biofilm communities of this opportunistic pathogen triggered by cystic fibrosis-induced hypoxia gradients at these sites [95]. The ability of these bacteria to form biofilms in anoxic environments was confirmed, over a glass surface [96]. Transcriptome and proteome analysis showed both *ccpA* and bacterial peroxidase were present in higher levels in biofilms isolated from cystic fibrosis patients [97]. Further transcriptomic analysis reported a 15-fold and 17-fold increase of *ccpA* expression in the presence of 2 % and 0.4 % of O_2, respectively, when compared to 20 % of O_2. These values are higher than the ones reported for the cytoplasmatic catalase encoding gene, *katA* (4.8-fold increase) [98], evidencing the importance of the bacterial peroxidase in such conditions.

In the case of *E. coli*, it has been shown that it can form biofilms under anoxic conditions, through the minimization of specific metabolic pathways, though this behavior was not generally seen before [99]. *E. coli* biofilm formation is slower in the absence of oxygen, but the extracellular polymer is unaltered. It was observed that *yhjA* gene has a higher expression level in biofilm compared to planktonic cells, and in both cases, it has a higher expression level under anoxic conditions (*yhjA* gene is upregulated in biofilm by 3.7-fold difference under anoxic medium when compared to planktonic cells) [99]. In fact, out of the major *E. coli* H_2O_2 scavengers identified (*katG*, *katE*, *ahpC*, *tpx*, *btuE* and *bcp*), *yhjA* is the one with the highest fold change [99]. Moreover, *E. coli* cells are more resistant to H_2O_2 stress and had a higher survival rate when grown in biofilms comparing to planktonic cells [100]. This agrees with YhjA being mainly produced anaerobically [63] and being involved in H_2O_2 reduction [60].

A. actinomycetemcomitans is a facultative anaerobic Gram-negative bacterium, capnophilic, known to be one of the causes for initiation of localized aggressive periodontitis in juveniles and adolescents [101]. The biofilm of this bacteria was characterized under aerobic conditions [102], a trait that does not favor the production of the bacterial peroxidase from this organism [56], which was in fact confirmed by the low levels of this protein. In addition, no significant change in bacterial peroxidase levels in biofilms compared to planktonic growth were observed in such conditions [102]. Thus, the expression level of *ccp* in biofilm formed under anaerobic conditions needs to be determined to understand the role of this enzyme under those conditions.

These findings, collectively, show that under anoxic environments bacterial peroxidases are upregulated in biofilm communities and that further studies using single knockout variants are required to establish and completely understand the role of these enzymes in such conditions.

3. Classical bacterial peroxidases

The first classical bacterial peroxidase was isolated from *P. aeruginosa* [103–105] and since then many other enzymes have been isolated and biochemically characterized from different microorganisms, such as *P. pantotrophus* [67], *Nitrosomonas europaea* [106], *Methylococcus capsulatus* BATH [107], *M. hydrocarbonoclasticus* 617 [68], *Pseudomonas stutzeri* [108,109], *N. gonorrhoeae* [76,110], *G. sulfurreducens* [61,111], and *S. oneidensis* [112].

As previously mentioned, classical bacterial peroxidases are homodimers with two *c*-type hemes as cofactors located in the periplasm. Though usually these enzymes are soluble in the periplasm, in some species they are reported to be membrane-anchored enzymes (Fig. 5), such as *N. gonorrhoeae* bacterial peroxidase, which is anchored to the outer-membrane by a lipid-modified cysteine [76].

The following sections will address the redox and spectroscopic properties, as well as its reductive activation and catalytic mechanism.

3.1. Heme coordination – Redox and spectroscopic properties

The clear difference in the reduction potential of the two *c*-type hemes of bacterial peroxidases was the basis for their designation since early studies. The C-terminus heme has a higher reduction potential ranging from + 226 mV [113] to + 420 mV [106], depending on the enzyme (Table 2), and it can receive electrons from sodium ascorbate, as well as from small electron donor proteins, such as *c*-type cytochromes and cupredoxins [114,115]. This heme has been named as high-potential or electron transferring heme (E heme). The N-terminus heme has a lower reduction potential ranging from - 330 mV [116] to - 220 mV [113] (Table 2) and it is able to bind exogenous substrates, in most of the enzymes, exclusively when the E heme is reduced [105,113,117–119]. This heme has been named as low-potential or peroxidatic heme (P heme).

3.1.1. Spectroscopic properties

Even though bacterial peroxidases are usually isolated with the two hemes oxidized, the difference between their reduction potential allows for a mixed-valence state with one heme reduced (E heme) and the other oxidized (P heme). These two oxidation states of the enzyme have been characterized using several spectroscopic techniques, such as magnetic circular dichroism (MCD), UV–visible, electron paramagnetic resonance (EPR) [106,109,120,121], Mössbauer [122], resonance Raman [123–126], and ^1H nuclear magnetic resonance (NMR) [113,127] (Table 1) spectroscopies.

The coordinating residues of the two hemes were identified through the analysis of the near-infrared magnetic circular dichroism (nIR-MCD) of *P. aeruginosa* bacterial peroxidase. In that study, it was reported that the enzyme in the oxidized stated had a bis-His coordinated P heme and the E heme was Met/His hexacoordinated [121], with the two hemes being low-spin at cryogenic temperatures. At room temperatures features of a high-spin species became evident, suggesting a high/low-spin equilibrium attributed to the weakly bound methionine to the E heme iron [121]. The charge-transfer band at around 620–640 nm present in the UV–visible spectrum of the oxidized bacterial peroxidase corroborates this high/low-spin equilibrium at E heme, as well as its heme methyl resonances at around 65-40 ppm in the ^1H NMR spectrum (Table 1).

Upon reduction of the E heme, the Soret band splits into two absorption bands, one with a maximum at 418–420 nm, corresponding to the ferrous E heme (Table 1), and a shoulder at 402–408 nm (Table 1), that arises from the low-spin ferric P heme. The charge-transfer band at 350–380 nm appears, while the one at 620–640 nm completely disappears in the case of *P. pantotrophus* [113] and *M. hydrocarbonoclasticus* [68] bacterial peroxidases (or it remains as a low intensity band, as observed in *N. gonorrhoeae* [110], *P. aeruginosa* [119], *P. stutzeri* [108] and *Rhodobacter capsulatus* [128] bacterial peroxidases, and in the two bacterial peroxidases from *G. sulfurreducens* [61,111]). Upon addition of calcium ions, a band, centered at 610–620 nm, is observed or becomes more intense. This absorption band is similar to the ones present in the high-spin penta-coordinated cytochrome *c'* [129], suggesting that P heme is high-spin penta-coordinated after reduction in the presence of calcium ions.

In fact, the P heme in the mixed-valence state enzyme is OH^-/His coordinated, given that it is in a temperature dependent high/low-spin equilibrium (low-spin EPR signal with *g*-values of 2.86, 2.36 and 1.53 at cryogenic temperatures [120], and nIR-MCD band at 1150 nm at room temperature [126,130–132]). In case P heme was H_2O/His coordinated, it would be high-spin (with

Table 2
Summary of the kinetic properties of classical bacterial peroxidases and related CCP_MauG related enzymes studied up-to-date and reduction potential of the hemes.

Organism	Electron Donor [a]	K_M H_2O_2 (µM)	K_M ED [b] (µM)	k_{cat} (s⁻¹)	pKa [c]	Reduction Potential (mV) vs. SHE			Ref.
						E heme	P heme	pH	
CcpA *Geobacter sulfurreducens*	ABTS²⁻ (3 mM)	6.2	–	15.5	–	–	–	–	[111,145]
MacA *Geobacter sulfurreducens*	ABTS²⁻ (3 mM)	38.5	–	0.46	–	–	– 237	7.5	[61]
Marinobacter hydrocarbonoclasticus 617	cytochrome c_{552} (38 µM)	–	122	460	–	–	–	–	[68]
Methylococcus capsulatus	cytochrome c_{555} (9 µM)	0.5	–	7.1	–	+ 432	– 254	7.0	[107]
Neisseria gonorrhoeae	ABTS²⁻ (3 mM)	4	–	79	5.9, 8.4	+ 310	– 190 / – 300	7.5	[110,168]
	LAz (10 µM)	0.4	–	39	5.1, 8.5				
Nitrosomonas europaea	Direct electrochemistry	–	–	–	6.5, 8.4	–	–	–	[106,117]
	horse heart cytochrome *c*	–	–	3	–	+ 450	- 260	7.0	
Paracoccus pantotrophus	cytochrome c_{550} (23 µM)	–	13	1417	–	+ 226	– 220	7.0	[113,138,162,167,175]
Pseudomonas aeruginosa	pseudoazurin (20 µM)	–	> 50	-	7.0				
	cytochrome c_{551} (13 µM)	6	88	143	4.4	+ 320	-330	7.0	[104,116,118,147,148,176]
	azurin	1	120	196	–	–	– 237	6.0	
Pseudomonas stutzeri	cytochrome c_{551} (7 µM)	1.8	54	338	–	–	–	–	[109]
Rhodobacter capsulatus	cytochrome c_2 (6 µM)	33	60	1060	–	+ 270	– 190 / – 310	7.5	[128,177]
Shewanella oneidensis	cytochrome c_5 (4 µM)	0.3	–	73		–	–	–	[112,158]
MauG *Paracoccus denitrificans*						– 159	– 240	7.4	[40]
MbnH *Methylosinus trichosporium*						– 38	– 257	7.5	[41]
BthA *Burkholdertia thailandesis*						– 121	– 165	7.0	[43]
RoxA						– 110	– 160	7.0	[53]

[a] Concentrations in parenthesis are the ones used to calculate the kinetic parameters presented (K_M and *kcat*) and pKa.
[b] K_M values for the electron donor are an estimative, as the concentrations used are below this value, except for cytochrome c_{550} from *P. pantotrophus*.
[c] pKa values determined by steady-state kinetics or protein-film voltammetry.

no temperature dependence and the charge-transfer band would be red shifted to 630–640 nm, similarly to what is observed for myoglobin in the ferric state [132,133]. The p*Ka* of this hydroxo group is proposed to be modulated by the calcium ion [110,134]. In the absence of calcium ion, the pKa is shifted to higher values, and the P heme becomes H_2O/His coordinated, with the visible band shifted towards 630–640 nm and a high-spin EPR signal is observed at cryogenic temperatures.

¹H NMR was also used to characterize the different oxidation states of bacterial peroxidases from *P. aeruginosa*, *P. stutzeri* and *P. pantotrophus*. In the spectrum of the oxidized bacterial peroxidase, the downfield resonances (51–58 ppm) are attributed to E heme in a high/low-spin equilibrium [135], as these resonances are lost upon reduction. The resonances at 28.3 and 33.2 ppm were attributed to the low-spin P heme and are downfield shifted upon E heme reduction (51–64 ppm), as the P heme becomes high-spin in the mixed-valence state [108,113,119,121,136].

Resonance Raman has also been used to characterize the oxidized and mixed-valence states of *P. pantotrophus* bacterial peroxidase [124,125], corroborating the spin state change observed in P heme, in the presence of calcium ions, upon reduction of the E heme. More recently, resonance Raman has been used to simply analyze the two oxidation states of *N. europaea* bacterial peroxidase wild-type and its H59G variant at cryogenic temperatures [126]. This study supported the proposal that P heme is low-spin at cryogenic temperatures, being coordinated by a hydroxo moiety in the mixed-valence state, as observed in the nIR-MCD, visible and EPR spectra of bacterial peroxidases.

These studies corroborate that formation of the high-spin mixed-valence state is dependent on the presence of calcium ions (Fig. 6). The different spectral properties of mixed-valence enzymes at cryogenic temperatures reflect the fact that these enzymes can be isolated with some level of endogenously

bound-Ca^{2+}, which is dependent on their production and isolation protocol, and in their calcium affinity. The use of EGTA to remove most bound calcium helped clarify their spectral features and the role of calcium in modulating these features [109,110,128,137] (Fig. 6C).

3.2. Activation mechanism

3.2.1. Dimerization and calcium binding site

In a study of the bacterial peroxidase from *P. pantotrophus* [138] it was observed that diluting the enzyme to suitable concentrations for kinetic assays led to a loss of catalytic activity over time, which was only partially recovered after re-concentration of the enzyme. By running the enzyme at different dilutions through molecular-exclusion chromatography it was shown that from higher to lower concentrations there is a shift in its apparent molecular weight from high to low, respectively (Fig. 6A). This indicates that the enzyme is in a monomer–dimer equilibrium in solution, which coupled with the kinetic data assigns the active form of the enzyme to the dimer and inactive form to the monomer [139]. Analytical ultracentrifugation studies of the same enzyme (at the same concentration, 10 µM) reported that in the as-isolated state it behaved mostly as a monomer and that after treatment with Ca^{2+} it becomes a dimer [139] (Fig. 6B). Additionally, differential scanning calorimetry also supported the role of calcium ions in enzyme dimerization due to an increase in its melting temperature in the presence of calcium ions when compared to the as-isolated form [139]. So, the active form of bacterial peroxidases as a dimer is not only dependent on enzyme concentration but also on the presence of calcium ions.

As mentioned, it is established that bacterial peroxidases can be produced and isolated with some level of endogenous bound-Ca^{2+} based on spectroscopic data. The calcium affinity varies between
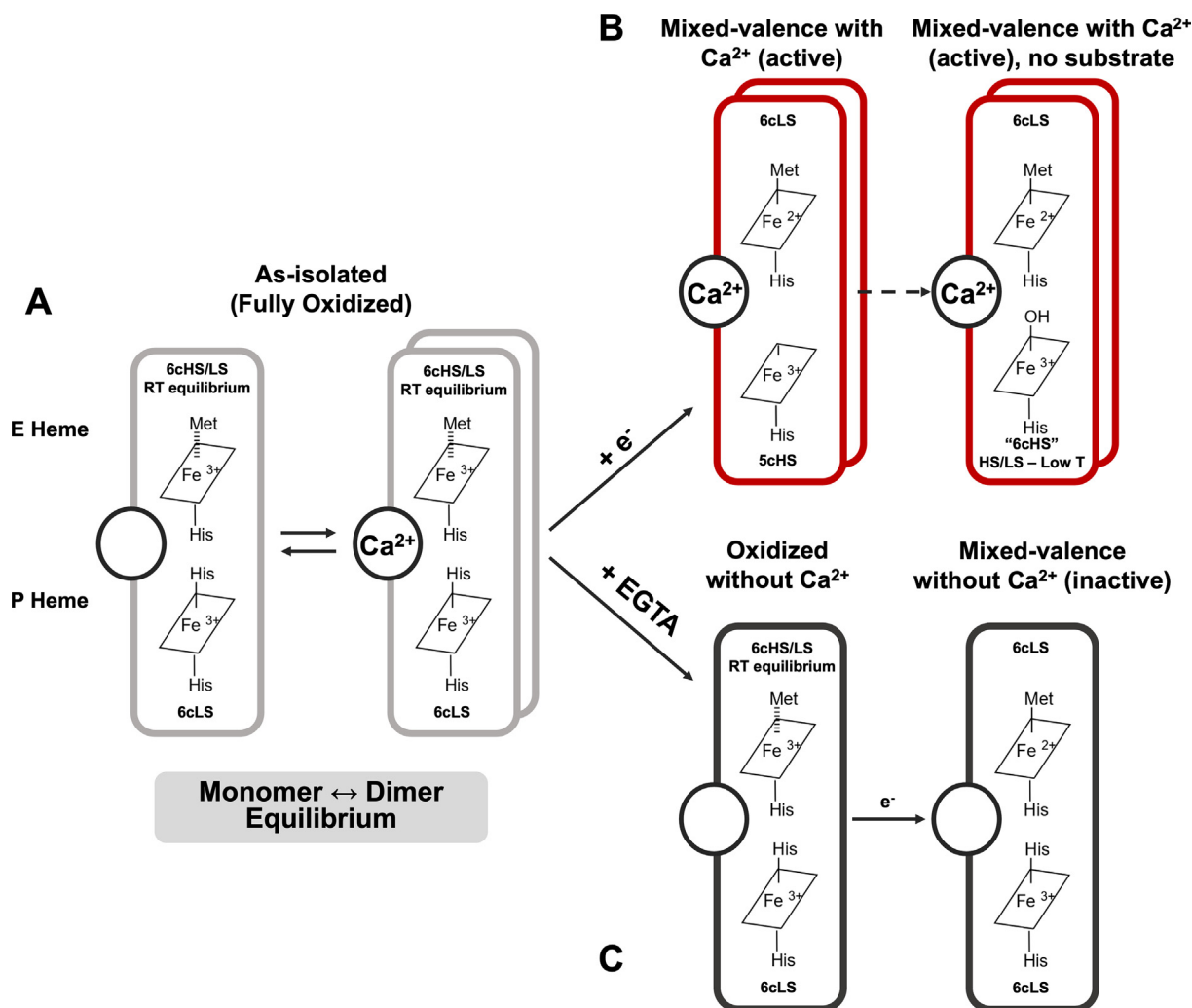
Fig. 6. Model for the activation mechanism of classical bacterial peroxidases. (**A**) The enzyme is isolated with both hemes in the oxidized state and hexacoordinated: E heme has a Met/His coordination and exists in a high/low-spin equilibrium (6cHS/LS) at room temperature due to the weakly bound Met (dashed line); the P heme has a bis-His coordination and exists in a low-spin state (6cLS). The monomer–dimer equilibrium typical of the isolated form of the enzyme, shifts to a fully dimer state in the presence of calcium ions. (**B**) Upon E heme reduction, in the presence of calcium ions, by an artificial or physiological electron donor, P heme's distal axial histidine is replaced by a hydroxyl group (OH$^-$/His coordination) and exists as 6cHS/LS at low temperature. This state of the enzyme is designated as active mixed-valence state and corresponds to the catalytic active form. In the presence of substrate, the distal axial position will be occupied by the substrate. (**C**) Removal of the calcium ions using a calcium chelator as EGTA shifts the monomer–dimer equilibrium to the monomeric state. In the mixed-valence state P heme remains bis-His coordinated, and this state is designated as inactive mixed-valence state.

enzymes, being highest for the enzyme in the mixed-valence state (low micromolar to nanomolar range) [110,137,140]. The crystallographic structures of bacterial peroxidases from *P. aeruginosa*, *N. europaea, P. pantotrophus, R. capsulatus, M. hydrocarbonoclasticus, G. sulfurreducens* and *S. oneidensis* confirm that these enzymes are homodimers with each monomer comprising two domains, each binding a *c*-type heme with one calcium ion bound in the interface between the two domains (Fig. 7A and 7B) [61,69,120,140–145]. The calcium ion is coordinated by four water molecules, two of which are H-bonded to propionate A of the E heme, and to the amide oxygen of three conserved residues (Asn93, Thr270 and Pro272, numbering from *P. pantotrophus* bacterial peroxidase) (Fig. 7D and 7E) [120,140,141].

3.2.2. Structural changes from inactive to active state

Kinetic studies on *P. aeruginosa* and *P. pantotrophus* bacterial peroxidases reported that when the catalytic assay was started by the addition of the oxidized enzyme to the reaction mixture containing the reduced electron donor and H_2O_2, a lag phase was observed prior to re-oxidation of the electron donor [138,146,147]. However, if the reaction was started by the addition of H_2O_2 to the reaction mixture, containing the enzyme and the reduced electron donor, the lag phase was absent but low catalytic activity was observed [138]. To attain maximum catalytic activity, the assay was started with the enzyme in the mixed-valence state, and calcium ions needed to be present in the reaction mixture [138].

These results suggested that in the oxidized state the catalytic center (P heme) is inaccessible to H_2O_2, and that there is a slow activation process dependent on the presence of calcium ions and reducing power to reduce the E heme – a reductive activation, that triggers the formation of the high-spin penta-coordinated P heme able to bind the substrate, H_2O_2 [116,130,138].

The comparison of crystallographic structures [61,69,75,111,120,141–143,145] of bacterial peroxidases in the inactive and mixed-valence state showed that the activation mechanism involved three structural steps (Fig. 7): 1) the E heme receives an electron and its D propionate group is protonated,
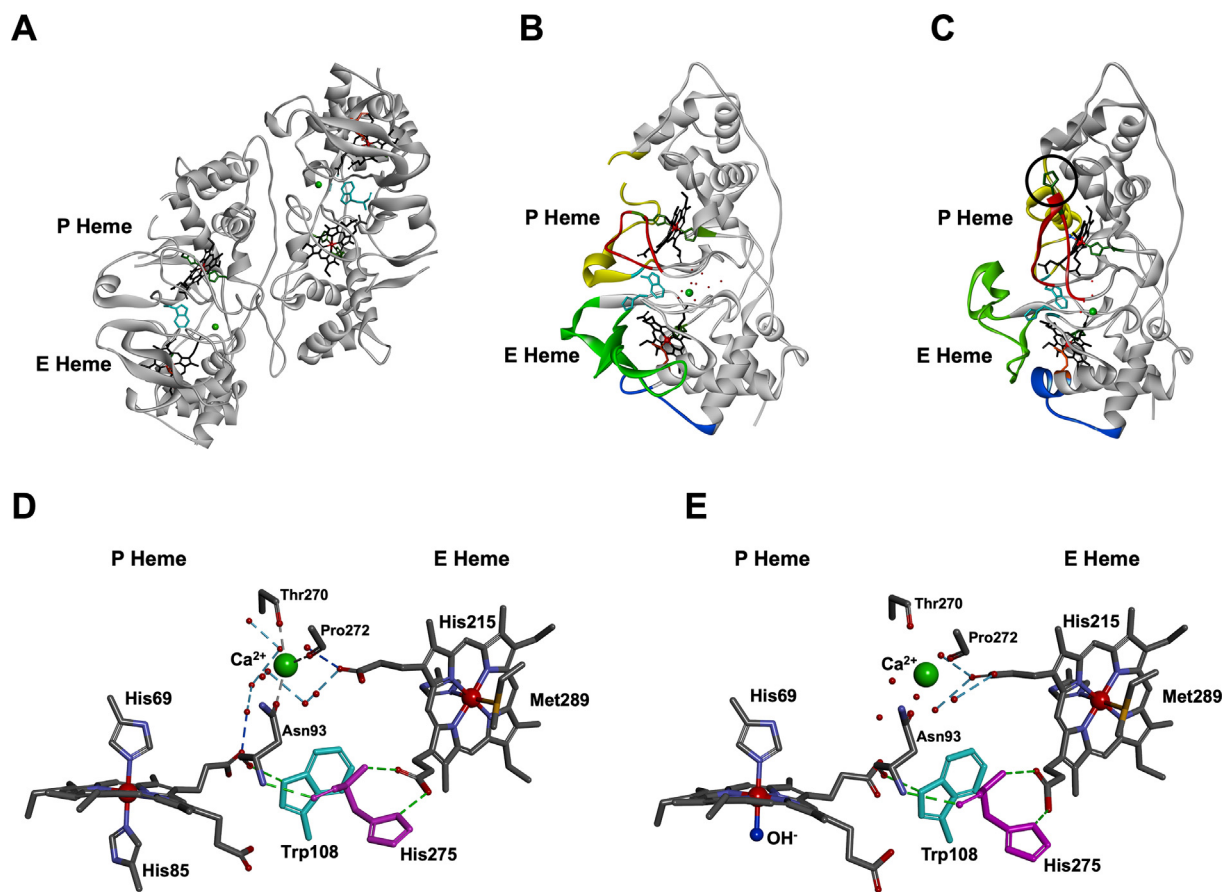
Fig. 7. Structural changes that occur upon reduction of E heme in *Paracoccus pantotrophus* bacterial peroxidase. (**A**) *Paracoccus pantotrophus* bacterial peroxidase in the oxidized state. In (**B**) and (**C**) are highlighted the four regions of the polypeptide chain that undergo structural changes described in the text, in the oxidized and mixed-valence enzyme, respectively. In (**D**) and (**E**) are shown the heme coordination and calcium ion for the oxidized and mixed-valence enzyme, respectively. In A, B and C the hemes are in black, histidine and methionine residues coordinating the heme iron are colored green and red, respectively and calcium ion as a green sphere. In D and E all atoms are colored by element, Trp108 and His275 side chains are colored in cyan and purple, respectively, calcium ion and OH⁻ are represented by a green and blue sphere, respectively. Figures were prepared in Discovery Studio Visualizer using the coordinates PDB ID 2C1U (A, B and D) and 2C1V (C and E).

which induces the movement of a loop between the heme domains; 2) this loop containing the axial histidine coordinating the P heme is relocated to the dimer interface leading to the loss of this axial ligand by P heme; 3) in the dimer interface, the loop stabilizes the dimer through π-stacking interactions between a tryptophan residue side chain, conserved in most bacterial peroxidases with the exception of *N. gonorrhoeae* and *M. capsulatus* [110], and the peptide bond of a glycine residue in the opposite monomer [120,141].

The loop stabilization at the dimer interface explains the absence of catalytic activity in a monomeric state. Nonetheless, a triple mutant (P75T/H81K/E84Q) in the loop containing the conserved tryptophan of *S. oneidensis* bacterial peroxidase was shown to be active in the mixed-valence state, though with a lower turnover number when compared to the wild-type [112].

Therefore, the role of the dimer seems to be only related with the stabilization of the active mixed-valence state of bacterial peroxidases and not directly with the catalysis itself [110].

3.3. Catalytic mechanism

The reduction of H_2O_2 to water takes place at the P heme and requires the transfer of two electrons. The electrons are delivered at E heme by electron shuttle proteins, allowing the enzyme to remain in its initial active form after the reaction. Eqs. (2) and (3) represent the peroxide reduction that takes place at P heme:

$$H_2O_2 + e^- + Fe^{3+} \rightarrow H_2O + Fe^{4+}=O \tag{2}$$

$$Fe^{4+}=O + e^+ + 2H^+ \rightarrow H_2O + Fe^{3+} \tag{3}$$
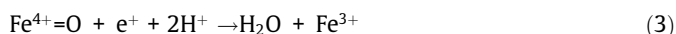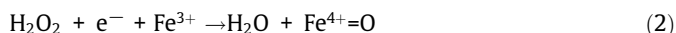
The catalytic mechanism considering the initial inactive state of the enzyme (dimeric fully oxidized with the calcium sites occupied, Fig. 8A), the pre-activation and intermediate species is represented in Fig. 8. In this proposed mechanism, the electrons are delivered by small electron shuttle proteins to the E heme that becomes reduced and promotes the formation of the ferric high-spin penta-coordinated P heme with a free position to bind H_2O_2 (Fig. 8B). The transfer of one electron from E heme to H_2O_2-bound P heme releases one water molecule and the intermediate $Fe^{4+}=O$ (oxoferryl species, Compound I, Fig. 8C) is formed. The donation of a second electron to E heme, subsequently transferred to P heme coupled with proton transfer forms the intermediate Fe^{3+}–OH (Compound II, Fig. 8D), and after another proton transfer the second water molecule is released.

Evidence of Compound I and Compound II came from spectroscopic studies using MCD and EPR on *P. aeruginosa* bacterial peroxidase [116,131,148,149]. Compound I presented spectroscopic features comparable to the oxyferryl species in peroxidases from horseradish and yeast, whereas Compound II was shown to be in an oxidation state equivalent to the inactive as-isolated enzyme, though with P heme still penta-coordinated. The restoration of the inactive fully oxidize state is not immediate as it is a slow process that occurs in the absence of reducing power (Fig. 8) [75].
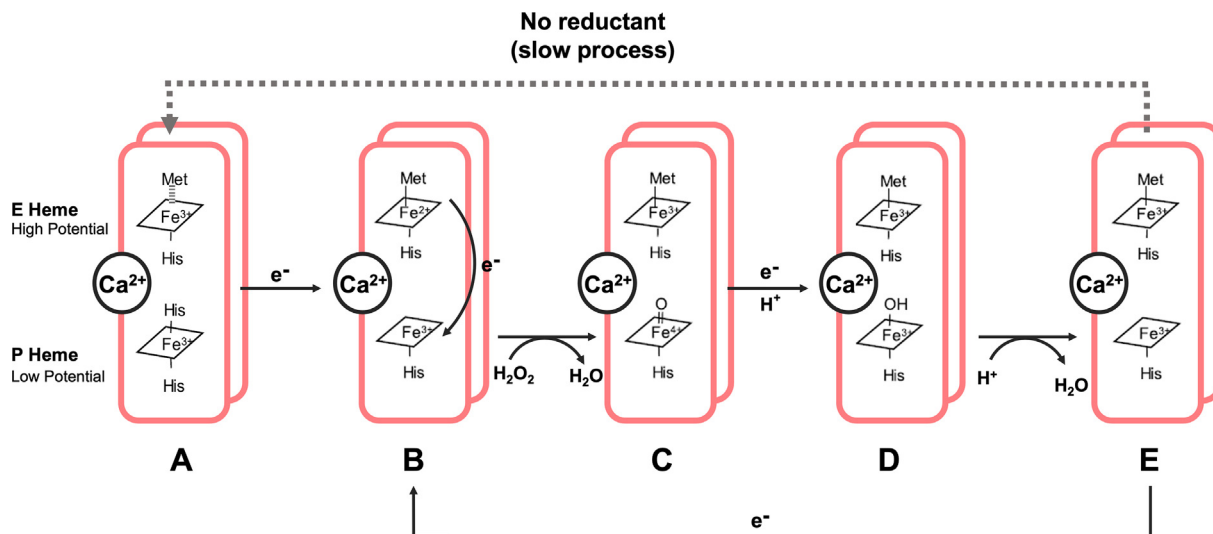
Fig. 8. Proposed catalytic mechanism of classical bacterial peroxidases. (**A**) Enzyme is a dimer due to the presence of calcium ions and has both hemes in the oxidized state. (**B**) Upon electron transfer from an external donor (artificial or physiological) the E heme becomes reduced, and the P heme loses its distal axial ligand and can bind the substrate, H_2O_2. (**C**) E heme transfers one electron to the P heme that reduces one H_2O_2 to one water molecule. The E heme returns to the oxidized state and a Fe^{4+}-oxo intermediate species (Compound I) is formed at the P heme. (**D**) A second electron, from an external donor and one proton from neighboring residue in the catalytic center, form Fe^{3+}–OH (Compound II). (**E**) A second proton is transferred to the P heme releasing a second water molecule. In the presence of substrate and enough reducing power the cycle goes back to (**B**), otherwise it will slowly return to (**A**).

In eukaryotic peroxidases (yeast cytochrome *c* peroxidase), the heterolytic cleavage O-O results in a porphyrin π-cation radical-Compound I. Compound I is stabilized through the reduction of porphyrin π-cation radical by a tryptophan residue, thus generating a tryptophan radical species [21,150]. The catalytic mechanism of bacterial peroxidases does not show formation of such radical species as the electron required to stabilize Compound I arises from the reduced E heme by electron shuttle proteins [151]. Nonetheless, studies on a variant of *P. aeruginosa* bacterial peroxidase (H71G) that lacked the P heme histidine ligand reported a red shift in the Soret band of the oxidized enzyme in the presence of excess of H_2O_2 [152,153]. A similar shift has been observed in the horseradish peroxidase, which was attributed to the formation of a tryptophan radical, and its presence has been confirmed by EPR [154]. Therefore, a "charge-hopping mechanism" for the intra-molecular electron transfer of bacterial peroxidase has been proposed to explain such a short-lived tryptophan-radical in the tryptophan residue between the two hemes, that precludes its experimental detection [152].

3.4. Intramolecular electron pathway

One of the key steps in the catalytic cycle of bacterial peroxidases is the two-electron transfer between E heme and P heme. However, the two hemes are distanced by around 20 Å, which does not favor direct electron transfer. Therefore, alternative mechanisms, such as charge hopping or electron tunneling have been proposed for the intramolecular electron pathway between the two hemes. Both mechanisms resort to the polypeptide chain to facilitate the process, however charge hopping enables electron transfer through longer distances due to the formation of transient radical centers along the chain [155–157]. Additionally, the charge hopping mechanism has been proposed to involve the side chains of tyrosine and tryptophan residues.

In bacterial peroxidases, the intramolecular electron pathway has not been thoroughly studied, though it is hypothesized that it consists of a hopping-type mechanism due to the presence of a tryptophan residue between the E heme and P heme (Trp108 in *P. pantotrophus* numbering, Fig. 7). This tryptophan residue acts

as a bridge between both hemes, with its indole ring located in between the propionate groups of E heme and P heme, at 10 Å from each [120,140,141]. Single variants of this residues resulted in an absence of catalytic activity, substantiating its importance in electron transfer [144,153]. Moreover, it also supports the previous data that reported the formation of a radical tryptophan species in *P. aeruginosa* bacterial peroxidase variants as an intermediate species [152,153].

3.5. Effect of pH in the catalytic activity

The proton donors for the second reaction are proposed to be Gln118 and Glu128 (numbering from *P. pantotrophus* bacterial peroxidase), conserved residues in P heme pocket. The mutation of these residues resulted in an inactive enzyme, even if in the mixed-valence state P heme was partially high-spin [144]. Other residues, Phe106, Pro112 and Met125 (numbering from *P. pantotrophus* bacterial peroxidase) have also been shown to be important for the catalysis by site-directed mutagenesis [144,158].

As proton donation has been proposed to be the rate-limiting step of the catalytic mechanism, to better understand the roles of the conserved P heme glutamate and glutamine residues, the pH dependency of the catalytic activity has been assessed. Bacterial peroxidases catalytic activity has a bell-shaped curve *versus* pH with an optimal activity around 7.5 with two pKa values. The heterolytic cleavage of O-O and formation of Compound I results from an acid/base catalysis by the distal histidine residue in eukaryotic peroxidases [159], with the chloroperoxidases family being the only hemic peroxidases with glutamate as acid/base catalyst [160]. The similarities in location and distance of ∼ 5 Å between the side chain carboxylate and the heme between the catalyst glutamate of chloroperoxidase and the conserved P heme glutamate bacterial peroxidase from *N. europaea* indicated that this residue takes part in the first reaction of the catalytic mechanism of bacterial peroxidases. As the glutamate needs to be deprotonated to assist the heterolytic cleavage, the lowest pKa value around pH 6.0 has been assign to this residue [110,142].

A *R. capsulatus* bacterial peroxidase variant in the glutamine residue (Gln118) showed no catalytic activity and in the bacterial

peroxidase from *P. pantotrophus* this glutamine was shown to be hydrogen bonded to a water molecule coordinating in the sixth position of the P heme in the mixed-valence state [141,144]. Thus, the highest pKa value around pH 8–10 could be associated with a proton transfer mediated by the glutamine residue in P heme's cavity for the release of the second water molecule.

3.6. Steady-state kinetic parameters

Steady-state kinetic parameters of bacterial peroxidase, obtained with its physiological or artificial redox partners as electron donors, are presented in Table 2. The highest catalytic activity reported for bacterial peroxidases with an artificial electron donor (ABTS^{2-}) is from *N. gonorrhoeae* with a K_M value of 4 μM and a turnover number (k_{cat}) of 70 s^{-1} at pH 7.0 [110]. Conversely, *G. sulfurreducens* MacA has the lowest reported catalytic activity with ABTS^{2-} as electron donor, and the optimal activity was observed at pH 5.5 with a K_M of 39 μM and k_{cat} of 0.46 s^{-1} [61].

The maximum catalytic activity with a physiological electron donor is reported for *R. capsulatus* bacterial peroxidase/cytochrome c_2 with a $K_M < 40$ μM and a turnover number (k_{cat}) of 1060 s^{-1}, at pH 7.5 [128].

3.7. Electron transfer complexes

3.7.1. Complex formation and intermolecular electron transfer

Few studies focused on the intermolecular electron transfer within bacterial peroxidase-donor protein complexes due to their transient nature required to achieve effective and high catalytic turnover numbers. Additionally, the electron transfer tends to be a very fast process that also depends on complex formation and dissociation rates. Regardless, resorting to several techniques, such as molecular docking simulations to generate structural models of the complexes [161], kinetic assays, microcalorimetry and NMR titrations it has been possible to obtain structural information about the nature of these complexes. In addition, electrochemical methods have provided the values for the intermolecular electron transfer rates [162,163].

The formation of these electron transfer complexes is mainly entropically driven due to the removal of water molecules from the complex interface, though in some cases these surface water molecules can take part in the stability of the complex and mediation of the electron transfer [164–166]. However, the absence of structural and mutagenesis data does not allow for a clear identification of the residues involved in the interface.

Small mono-hemic *c*-type cytochromes or type-1 copper proteins, such as azurin and pseudoazurin are the typical physiological electron donors of bacterial peroxidases [114,115,167,168]. NMR titrations and bioinformatic studies (molecular docking or electrostatic surface prediction) have demonstrated that the character of bacterial peroxidase-redox partner interaction is not universal. In the case of bacterial peroxidases from *P. pantotrophus* and *R. capsulatus* the electron transfer complex has an electrostatic nature [115,167,169]. *P. pantotrophus* bacterial peroxidase has two physiological electron donors, pseudoazurin and cytochrome c_{550} [115,162,165–167,170]. The surface of cytochrome c_{550} involved in the binding comprehends a ring of lysine residues surrounding a hydrophobic patch with the solvent exposed heme edge in the middle [115,165,170]. For *P. pantotrophus* pseudoazurin the binding surface involves the type-I copper coordinating histidine, the proposed electron entry site, and its surrounding ring of lysine residues, as chemical shift perturbation of these residues was observed in the presence of the enzyme [167]. Similarly to *P. pantotrophus* cytochrome c_{550}, *R. capsulatus* cytochrome c_2 has 14

lysine residues surrounding the solvent exposed heme edge, with 6 of these residues being proposed to interact with the negatively charged residues surrounding the hydrophobic patch involving the solvent exposed E heme edge of the bacterial peroxidase from the same organism. The importance of these residues was corroborated by the observation that the loss of some of the lysine residues lead to complex disruption [169].

In contrast, the electron transfer complex of bacterial peroxidases from *M. hydrocarbonoclasticus* and *N. gonorrhoeae* are hydrophobic in nature [68,168,171]. For *N. gonorrhoeae* lipid-modified azurin (Laz), chemical shift mapping identified residues located within the hydrophobic patch surrounding the type-1 copper center, coupled to the hydrophobic character of the surface encompassing the E heme of this enzyme, supports the hydrophobic nature of this complex [168]. Additionally, unlike *P. pantotrophus* pseudoazurin, *N. gonorrhoeae* Laz does not have a ring of lysine residues surrounding the hydrophobic patch of the type-1 copper center [171]. The *M. hydrocarbonoclasticus* 617 bacterial peroxidase-cytochrome c_{552} complex is proposed to have a hydrophobic character as both proteins have very few charged residues in its surface [143,172]. In addition, the mediated hydrogen peroxide reduction is not affected by the presence of NaCl (up to 600 mM NaCl) [68], which would not be the case if it was an electrostatic complex [115,167]. This property might be an advantage considering the habitat of this marine organism.

The complex stoichiometry and dissociation constants have only been reported for *P. pantotrophus* bacterial peroxidase and *G. sulfurreducens* MacA, both having a 1:1 stoichiometry [82,115,165,167,170]. ^{1}H NMR by following heme methyl resonances of *G. sulfurreducens* MacA/PpcA complex reported two dissociation constants for MacA associated with a first binding event (K_{D1} = 113 μM) followed by a second binding event (K_{D2} = 879–1243 μM), proposing that initially PpcA will exclusively interact with the primary binding site and only after this being fully-occupied, PpcA will bind to the secondary site [82]. Microcalorimetry and ultracentrifugation studies of *P. pantotrophus* bacterial peroxidase/pseudoazuin and bacterial peroxidase/cytochrome c_{550} complexes suggested the existence of a single binding site for these electron donor proteins on the bacterial peroxidase, with K_D in the micromolar range (2–20 μM), respectively [115,165,167]. Moreover, pseudoazurin and cytochrome c_{550} bind bacterial peroxidase at the same site [139,165–167].

4. Non-classical bacterial peroxidases

The non-classical bacterial peroxidases are tri-hemic enzymes, with a C-terminus domain homologous to the classical bacterial peroxidase and an additional domain at the N-terminus that also binds a *c*-type heme (named NT-domain). The gene encoding for these enzymes is found in the genome of known pathogenic (Fig. 3) and opportunistic bacteria. YhjA from *E. coli* [60,134], PerC from *Z. mobilis* [59] and QPO from *A. actinomycetemcomitans* [55–58] are the only non-classical bacterial peroxidases isolated and characterized up to now. Both YhjA and PerC have a putative transmembrane helix in the N-terminus, while QPO is confirmed to be a membrane protein, with the three enzymes being classified as quinol-dependent bacterial peroxidases.

The analysis of the primary sequence of these enzymes and the structure of *E. coli* YhjA shows the conserved features of classical bacterial peroxidases: (i) the essential tryptophan, that mediates the electron transfer between E and P heme, (ii) calcium binding residues, and (iii) the conserved glutamine and glutamate residues involved in the catalytic cycle [134] (Fig. 9). However, no distal histidine ligand for the P heme was identified, and spectroscopic data
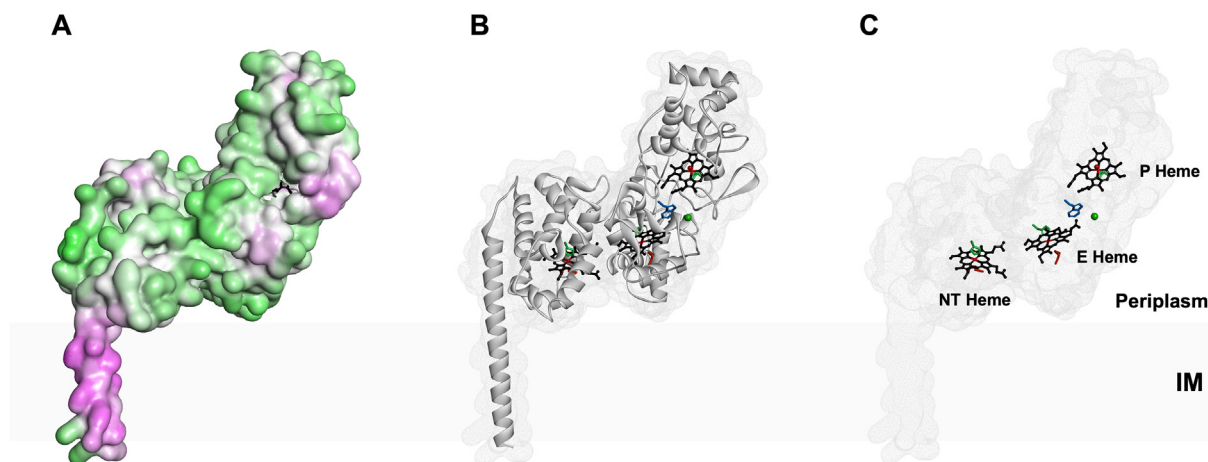
Fig. 9. Model of the non-classical bacterial peroxidases. *Escherichia coli* YhjA is shown with its surface colored from non-hydrophobic (green) to hydrophobic (magenta) residues in (**A**), and the structural arrangement of the hemes, conserved tryptophan and calcium ion is shown in (**B**) and (**C**). The structure of YhjA was obtained using alphafold2 colab [173,174]. E and P heme were positioned according with the structure superimposition with the coordinates 2C1V, and NT heme was oriented so that it was coordinated by its axial ligands and the cysteines were at a distance to form a thioether bond with the vinyls of the heme. Figures were prepared in Discovery Studio Vizualizer.

showed that this heme is OH⁻/His coordinated [55,134], and thus is ready to bind the substrate (Fig. 9C).

The additional *c*-type heme domain has low sequence homology with other *c*-type cytochromes, and its distal axial ligand is proposed to be a methionine based on the spectroscopic characterization of the full-length enzyme and isolated NT domain [134], and in the model Met125 is positioned in the correct orientation to coordinate NT heme.

The isolated soluble domain of *E. coli* bacterial peroxidase confirms that YhjA is a monomeric trihemic enzyme even in the presence of calcium ions or when reduced with sodium ascorbate [134], unlike classical bacterial peroxidases [115]. In fact, the thermogram of *E. coli* YhjA shows two transitions, interpreted as the unfolding of two independent domains, and confirmed the analysis of its apparent molecular weight in solution [134].

The UV–visible spectrum of these enzymes in the oxidized state presents the typical cytochrome *c* Soret absorption band around 410 nm, and two additional absorption bands: (i) at 620 nm, band characteristic of the presence of high-spin hemes, and (ii) at 695 nm, a weak band attributed to a Met axial ligand [134]. The spectra of the ascorbate-reduced enzyme show three bands with maxima absorption at 419 nm, 524 nm and 553 nm, which are the Soret, beta and alpha bands, respectively [55,134].

The reduction potential of the three hemes have been determined for YhjA by potentiometric titrations at pH 7.5 to be − 170 mV (P), + 133 mV (NT) and + 210 mV (E), and are more negative than the ones reported for QPO, +67 mV (P), +156 mV (NT) and + 290 mV (E), at the same pH [55,134]. This is the only report of a positive potential of the P heme in bacterial peroxidases (Table 2). The lower reduction potential of NT heme compared to E heme is coherent with the proposed electron transfer from the quinone pool to the NT heme, and from NT heme to the E heme, in both bacteria.

Although neither QPO nor YhjA seems to require reductive activation, the latter requires the presence of calcium ions for maximum activity [134]. The K_M for H_2O_2 is >10-fold lower for QPO than for YhjA (39 μM and 0.6 mM, respectively), as *E. coli* YhjA is a poor peroxidase *in vitro* when using hydroquinone as the electron donor [134]. These results are explained by the fact that QPO used in the assays was in its native form, *i.e.*, with the transmembrane domain, while YhjA lacked this domain, which is proposed to be involved in the electron transfer pathway from the quinone pool.

Moreover, menaquinol, the putative physiological electron donor of YhjA [60], was not used in the assays. Nevertheless, the K_M estimated *in vivo* of 5 μM for this enzyme supports this explanation [60].

PerC from *Z. mobilis* was showed to have an impact in the membrane NADH peroxidase activity in aerobic growth, and sensitivity of cells to exogenous hydrogen peroxide, as seen with a *perC* knockout strain [59]. In the same work it was established that PerC does not receive electrons from the *bc₁* complex, and thus it is more likely to receive electrons from the quinol pool, as proposed.

Furthermore, both YhjA and QPO attain maximum activity at pH 7.0–7.5, and their catalytic activity have a bell-shaped pH dependence profile [55,134].

QPO follows a Ping Pong Bi Bi catalytic mechanism using 1-ubiquinol as electron donor and enzyme inactivation was observed at high concentrations of H_2O_2 [58]. In the case of YhjA, the P heme forms an oxoferryl radical in the oxidized form that is capable of binding the substrate, as observed through visible spectroscopy [134].

The elucidation of the function of the third heme on the N-terminus domain, as well as the transmembrane domain have yet to be achieved. To do so, three-dimensional structures of the full-length trihemic bacterial peroxidases should be attained, as well as site-directed mutagenesis to understand its impact on the catalytic activity.

5. Concluding remarks

The CCP_MauG family encompasses enzymes with different functions, most of which still to identify. This di(tri)-hemic enzymes catalyze proton-coupled reductions of substrates at a *c*-type heme, having as intermediate species a Fe^{4+}oxoferryl, and relying on the intramolecular electron transfer from the other *c*-type hemes. In the case of bacterial peroxidases, the substrate is hydrogen peroxide, and the electrons come from small electron shuttle proteins or from the quinol pool.

Most of the biochemical and structural studies of bacterial peroxidases are from the classical enzymes, though their catalytic cycle and intramolecular electron transfer pathway are still poorly characterized. Further work is needed to identify the intermediate species and the origin of the two protons required for the complete

reduction of hydrogen peroxide (either from a residue or a nearby solvent molecule). Although tri-hemic enzymes are a challenge to obtain in large amounts from *E. coli*, their three-dimensional structure can provide clues to understand the role of the additional heme binding domain, and enzymatic assays performed under more physiological conditions will clarify their affinity to hydrogen peroxide.

The physiological role of these enzymes in anaerobic proliferation, by enabling the use of H_2O_2 as a terminal electron acceptor must be explored, as well as their involvement in biofilm communities. Moreover, these enzymes play a vital role in pathogenicity under anaerobic conditions, which makes them important virulence traits, and thus interesting therapeutic targets to be explored.

Author contributions

SRP planned the manuscript with contributions from DB. DB, RO and SRP wrote the manuscript.

Data availability

Data will be made available on request.

Declaration of Competing Interest

The authors declare that they have no known competing financial interests or personal relationships that could have appeared to influence the work reported in this paper.

Acknowledgments

References

[1] K.J. Dietz, Mol. Cells 39 (2016) 20–25.
[2] S.O. Kang, M.K. Kwak, J. Microbiol. Biotechnol. 31 (2021) 79–91.
[3] C.S. Nobrega, S.R. Pauleta, Adv. Microb. Physiol. 74 (2019) 415–464.
[4] C. Leblanc, H. Vilter, J.B. Fournier, L. Delage, P. Potin, E. Rebuffet, G. Michel, P.L. Solari, M.C. Feiters, M. Czjzek, Coord. Chem. Rev. 301–302 (2015) 134–146.
[5] C.C. McLauchlan, H.A. Murakami, C.A. Wallace, D.C. Crans, J. Inorg. Biochem. 186 (2018) 267–279.
[6] Z. Chen, Coord. Chem. Rev. 457 (2022).
[7] S. Kawasaki, M. Ono, Y. Watamura, Y. Sakai, T. Satoh, T. Arai, J. Satoh, Y. Niimura, FEBS Lett. 581 (2007) 2460–2464.
[8] M.L. Caldas Nogueira, A.J. Pastore, V.L. Davidson, Arch. Biochem. Biophys. 705 (2021).
[9] E.D. Coulter, N.V. Shenvi, D.M. Kurtz Jr., Biochem. Biophys. Res. Commun. 255 (1999) 317–323.
[10] M.V. Weinberg, F.E. Jenney Jr., X. Cui, M.W. Adams, J. Bacteriol. 186 (2004) 7888–7895.
[11] F. deMare, D.M. Kurtz Jr., P. Nordlund, Nat. Struct. Biol. 3 (1996) 539–546.
[12] B.D. Dillard, J.M. Demick, M.W. Adams, W.N. Lanzilotta, J. Biol. Inorg. Chem. 16 (2011) 949–959.

[13] M. Zamocky, C. Jakopitsch, P.G. Furtmuller, C. Dunand, C. Obinger, Proteins 72 (2008) 589–605.
[14] M. Zamocky, S. Hofbauer, I. Schaffner, B. Gasselhuber, A. Nicolussi, M. Soudi, K.F. Pirker, P.G. Furtmuller, C. Obinger, Arch. Biochem. Biophys. 574 (2015) 108–119.
[15] N.B. Loughran, B. O'Connor, C. O'Fagain, M.J. O'Connell, BMC Evol. Biol. 8 (2008) 101.
[16] N. Bakalovic, F. Passardi, V. Ioannidis, C. Cosio, L. Penel, L. Falquet, C. Dunand, Phytochemistry 67 (2006) 534–539.
[17] L.M. Shannon, E. Kay, J.Y. Lew, J. Biol. Chem. 241 (1966) 2166–2172.
[18] K.G. Paul, W. v. Studnitz, G. Bergson, A. Grönvall, B. Zaar, E. Diczfalusy,, Acta Chem. Scand. 12 (1958) 1312–1318.
[19] A.M. Altschul, R. Abrams, T.R. Hogness, J. Biol. Chem. 136 (1940) 777–794.
[20] B.C. Finzel, T.L. Poulos, J. Kraut, J. Biol. Chem. 259 (1984) 13027–13036.
[21] J.E. Erman, L.B. Vitello, Biochim. Biophys. Acta 1597 (2002) 193–220.
[22] G.I. Berglund, G.H. Carlsson, A.T. Smith, H. Szoke, A. Henriksen, J. Hajdu, Nature 417 (2002) 463–468.
[23] A. Kumar, P.K. Arora, Front. Environ. Sci. 10 (2022).
[24] M. Sundaramoorthy, M.H. Gold, T.L. Poulos, J. Inorg. Biochem. 104 (2010) 683–690.
[25] M. Hofrichter, R. Ullrich, M.J. Pecyna, C. Liers, T. Lundell, Appl. Microbiol. Biotechnol. 87 (2010) 871–897.
[26] Y. Chang, D. Yang, R. Li, T. Wang, Y. Zhu, Molecules 26 (2021).
[27] A.O. Falade, U.U. Nwodo, B.C. Iweriebor, E. Green, L.V. Mabinya, A.I. Okoh, Microbiologyopen 6 (2017) e00394.
[28] Y. Sugano, T. Yoshida, Int. J. Mol. Sci. 22 (2021).
[29] T. Yoshida, Y. Sugano, Arch. Biochem. Biophys. 574 (2015) 49–55.
[30] T. Yoshida, H. Tsuge, H. Konno, T. Hisabori, Y. Sugano, FEBS J. 278 (2011) 2387–2394.
[31] A.K. Singh, M.L. Smith, S. Yamini, P.I. Ohlsson, M. Sinha, P. Kaur, S. Sharma, J.A. Paul, T.P. Singh, K.G. Paul, Protein J. 31 (2012) 598–608.
[32] A.K. Singh, R.P. Kumar, N. Pandey, N. Singh, M. Sinha, A. Bhushan, P. Kaur, S. Sharma, T.P. Singh, J. Biol. Chem. 285 (2010) 1569–1576.
[33] P.K. Singh, S. Pandey, C. Rani, N. Ahmad, V. Viswanathan, P. Sharma, P. Kaur, S. Sharma, T.P. Singh, J. Biol. Inorg. Chem. 26 (2021) 149–159.
[34] J. Zeng, R.E. Fenna, J. Mol. Biol. 226 (1992) 185–207.
[35] T.J. Fiedler, C.A. Davey, R.E. Fenna, J. Biol. Chem. 275 (2000) (1971) 11964–111961.
[36] M. Hofrichter, R. Ullrich, Appl. Microbiol. Biotechnol. 71 (2006) 276–288.
[37] S. Kumar, G. Stecher, M. Li, C. Knyaz, K. Tamura, Mol. Biol. Evol. 35 (2018) 1547–1549.
[38] Y. Wang, M.E. Graichen, A. Liu, A.R. Pearson, C.M. Wilmot, V.L. Davidson, Biochemistry 42 (2003) 7318–7325.
[39] Y. Wang, X. Li, L.H. Jones, A.R. Pearson, C.M. Wilmot, V.L. Davidson, J. Am. Chem. Soc. 127 (2005) 8258–8259.
[40] X. Li, M. Feng, Y. Wang, H. Tachikawa, V.L. Davidson, Biochemistry 45 (2006) 821–828.
[41] G.E. Kenney, L.M.K. Dassama, A.C. Manesis, M.O. Ross, S. Chen, B.M. Hoffman, A.C. Rosenzweig, J. Biol. Chem. 294 (2019) 16141–16151.
[42] A.C. Manesis, R.J. Jodts, B.M. Hoffman, A.C. Rosenzweig, PNAS 118 (2021).
[43] K. Rizzolo, S.E. Cohen, A.C. Weitz, M.M. Lopez Munoz, M.P. Hendrich, C.L. Drennan, S.J. Elliott, Nat. Commun. 10 (2019) 1101.
[44] K. Rizzolo, A.C. Weitz, S.E. Cohen, C.L. Drennan, M.P. Hendrich, S.J. Elliott, J. Am. Chem. Soc. 142 (2020) (1982) 11978–111971.
[45] A.C. Weitz, S. Biswas, K. Rizzolo, S. Elliott, E.L. Bominaar, M.P. Hendrich, Inorg. Chem. 59 (2020) 10223–10233.
[46] C. Zapata, B. Paillavil, R. Chavez, P. Alamos, G. Levican, FEMS Microbiol. Ecol. 93 (2017).
[47] A. Ferrer, B. Bunk, C. Sproer, N. Biedendieck, M. Valdes, M. Jahn, D. Jahn, O. Orellana, G. Levican, J. Biotechnol. 222 (2016) 21–22.
[48] S. Lim, J.H. Jung, L. Blanchard, A. de Groot, FEMS Microbiol. Rev. 43 (2019) 19–52.
[49] K.S.T. Frade, A.C.P. Fernandes, C.M. Silveira, C. Frazao, E. Moe, Acta Crystallogr F Struct Biol Commun 74 (2018) 419–424.
[50] G.D. Wiens, S.E. LaPatra, T.J. Welch, C. Rexroad 3rd, D.R. Call, K.D. Cain, B.R. LaFrentz, B. Vaisvil, D.P. Schmitt, V. Kapatral, Genome Announc. 2 (2014).
[51] H.A. Levipan, J. Quezada, R. Avendano-Herrera, Front. Microbiol. 9 (2018) 18.
[52] R. Braaz, W. Armbruster, D. Jendrossek, Appl. Environ. Microbiol. 71 (2005) 2473–2478.
[53] G. Schmitt, G. Seiffert, P.M.H. Kroneck, R. Braaz, D. Jendrossek, Microbiology (Reading) 156 (2010) 2537–2548.
[54] J. Seidel, G. Schmitt, M. Hoffmann, D. Jendrossek, O. Einsle, PNAS 110 (2013) 13833–13838.
[55] H. Yamada, E. Takashima, K. Konishi, FEBS J. 274 (2007) 853–866.
[56] E. Takashima, K. Konishi, FEMS Microbiol. Lett. 286 (2008) 66–70.
[57] E. Takashima, H. Yamada, T. Yamashita, K. Matsushita, K. Konishi, FEMS Microbiol. Lett. 302 (2010) 52–57.
[58] T. Abe, T. Kawarai, Y. Takahashi, K. Konishi, J. Biochem. 161 (2017) 513–520.
[59] E. Balodite, I. Strazdina, N. Galinina, S. McLean, R. Rutkis, R.K. Poole, U. Kalnienieks, Microbiology 160 (2014) 2045–2052.
[60] M. Khademian, J.A. Imlay, PNAS 114 (2017) E6922–E6931.
[61] J. Seidel, M. Hoffmann, K.E. Ellis, A. Seidel, T. Spatzal, S. Gerhardt, S.J. Elliott, O. Einsle, Biochemistry 51 (2012) 2747–2756.
[62] L.K. Bingham-Ramos, D.R. Hendrixson, Infect. Immun. 76 (2008) 1105–1114.
[63] J.D. Partridge, R.K. Poole, J. Green, Microbiology 153 (2007) 1499–1509.
[64] C.D. Herren, E.R. Rocha, C.J. Smith, Gene 316 (2003) 167–175.

[65] S. Lissenden, S. Mohan, T. Overton, T. Regan, H. Crooke, J.A. Cardinale, T.C. Householder, P. Adams, C.D. O'Conner, V.L. Clark, H. Smith, J.A. Cole, Mol. Microbiol. 37 (2000) 839–855.

[66] R.J. Van Spanning, A.P. De Boer, W.N. Reijnders, H.V. Westerhoff, A.H. Stouthamer, J. Van Der Oost, Mol. Microbiol. 23 (1997) 893–907.

[67] C.F. Goodhew, I.B. Wilson, D.J. Hunter, G.W. Pettigrew, Biochem. J. 271 (1990) 707–712.

[68] T. Alves, S. Besson, L.C. Duarte, G.W. Pettigrew, F.M.F. Girio, B. Devreese, I. Vandenberghe, J. Van Beeumen, G. Fauque, I. Moura, Biochim. Biophys. Acta 1434 (1999) 248–259.

[69] B. Schutz, J. Seidel, G. Sturm, O. Einsle, J. Gescher, Appl. Environ. Microbiol. 77 (2011) 6172–6180.

[70] L.C. Seaver, J.A. Imlay, J. Biol. Chem. 279 (2004) 48742–48750.

[71] N.S. Chandel, D.S. McClintock, C.E. Feliciano, T.M. Wood, J.A. Melendez, A.M. Rodriguez, P.T. Schumacker, J. Biol. Chem. 275 (2000) 25130–25138.

[72] A. Sen, J.A. Imlay, Front. Immunol. 12 (2021).

[73] B.A. Lazazzera, H. Beinert, N. Khoroshilova, M.C. Kennedy, P.J. Kiley, J. Biol. Chem. 271 (1996) 2762–2768.

[74] J.C. Crack, N.E. Le Brun, Coord. Chem. Rev. 448 (2021).

[75] G.W. Pettigrew, A. Echalier, S.R. Pauleta, J. Inorg. Biochem. 100 (2006) 551–567.

[76] S. Turner, E. Reid, H. Smith, J. Cole, Biochem. J. 373 (2003) 865–873.

[77] N.V. Balashova, D.H. Park, J.K. Patel, D.H. Figurski, S.C. Kachlany, Infect. Immun. 75 (2007) 4490–4497.

[78] A.J. van Winkelhoff, J. Slots, Periodontol 2000 (20) (1999) 122–135.

[79] N.V. Balashova, J.A. Crosby, L. Al Ghofaily, S.C. Kachlany, Infect. Immun. 74 (2006) 2015–2021.

[80] E.T. Lally, R.B. Hill, I.R. Kieba, J. Korostoff, Trends Microbiol. 7 (1999) 356–361.

[81] D.R. Hendrixson, V.J. DiRita, Mol. Microbiol. 52 (2004) 471–484.

[82] J.M. Dantas, A. Brausemann, O. Einsle, C.A. Salgueiro, FEBS Lett. 591 (2017) 1657–1666.

[83] M. Aklujkar, M.V. Coppi, C. Leang, B.C. Kim, M.A. Chavan, L.A. Perpetua, L. Giloteaux, A. Liu, D.E. Holmes, Microbiology 159 (2013) 515–535.

[84] B.C. Kim, D.R. Lovley, FEMS Microbiol. Lett. 286 (2008) 39–44.

[85] E.S. Shelobolina, M.V. Coppi, A.A. Korenevsky, L.N. DiDonato, S.A. Sullivan, H. Konishi, H. Xu, C. Leang, J.E. Butler, B.C. Kim, D.R. Lovley, BMC Microbiol. 7 (2007) 16.

[86] J.E. Butler, F. Kaufmann, M.V. Coppi, C. Nunez, D.R. Lovley, J. Bacteriol. 186 (2004) 4042–4045.

[87] C.F. Goodhew, A.B. elKurdi, G.W. Pettigrew, Biochim. Biophys. Acta 933 (1988) 114–123.

[88] J.A. Imlay, Environ. Microbiol. 21 (2019) 521–530.

[89] L. Hall-Stoodley, P. Stoodley, Cell. Microbiol. 11 (2009) 1034–1043.

[90] R.M. Donlan, J.W. Costerton, Clin. Microbiol. Rev. 15 (2002) 167–193.

[91] L.L. Greiner, J.L. Edwards, J. Shao, C. Rabinak, D. Entz, M.A. Apicella, Infect. Immun. 73 (2005) 1964–1970.

[92] K.L. Seib, H.J. Wu, Y.N. Srikhanta, J.L. Edwards, M.L. Falsetta, A.J. Hamilton, T.L. Maguire, S.M. Grimmond, M.A. Apicella, A.G. McEwan, M.P. Jennings, Mol. Microbiol. 63 (2007) 54–68.

[93] M.L. Falsetta, T.B. Bair, S.C. Ku, R.N. Vanden Hoven, C.T. Steichen, A.G. McEwan, M.P. Jennings, M.A. Apicella, Infect. Immun. 77 (2009) 3522–3532.

[94] N.J. Phillips, C.T. Steichen, B. Schilling, D.M. Post, R.K. Niles, T.B. Bair, M.L. Falsetta, M.A. Apicella, B.W. Gibson, PLoS One 7 (2012) e38303.

[95] D. Worlitzsch, R. Tarran, M. Ulrich, U. Schwab, A. Cekici, K.C. Meyer, P. Birrer, G. Bellon, J. Berger, T. Weiss, K. Botzenhart, J.R. Yankaskas, S. Randell, R.C. Boucher, G. Doring, J. Clin. Invest. 109 (2002) 317–325.

[96] S.S. Yoon, R.F. Hennigan, G.M. Hilliard, U.A. Ochsner, K. Parvatiyar, M.C. Kamani, H.L. Allen, T.R. DeKievit, P.R. Gardner, U. Schwab, J.J. Rowe, B.H. Iglewski, T.R. McDermott, R.P. Mason, D.J. Wozniak, R.E. Hancock, M.R. Parsek, T.L. Noah, R.C. Boucher, D.J. Hassett, Dev. Cell 3 (2002) 593–603.

[97] C. Hoboth, R. Hoffmann, A. Eichner, C. Henke, S. Schmoldt, A. Imhof, J. Heesemann, M. Hogardt, J Infect Dis 200 (2009) 118–130.

[98] C. Alvarez-Ortega, C.S. Harwood, Mol. Microbiol. 65 (2007) 153–165.

[99] B. Bayramoglu, D. Toubiana, O. Gillor, FEMS Microbiol. Lett. 364 (2017).

[100] W. Jakubowski, B. Walkowiak, Braz. Arch. Biol. Technol. 58 (2015) 300–308.

[101] D.H. Fine, K. Markowitz, D. Furgang, K. Fairlie, J. Ferrandiz, C. Nasri, M. McKiernan, J. Gunsolley, J. Clin. Microbiol. 45 (2007) 3859–3869.

[102] A. Llama-Palacios, O. Potupa, M.C. Sanchez, E. Figuero, D. Herrera, M. Sanz, J. Proteome Res. 16 (2017) 3158–3167.

[103] N. Ellfolk, R. Soininen, Acta Chem. Scand. 24 (1970) 2126–2136.

[104] R. Soininen, N. Ellfolk, Acta Chem. Scand. 26 (1972) 861–872.

[105] R. Soininen, N. Ellfolk, Acta Chem. Scand. 27 (1973) 35–46.

[106] D.M. Arciero, A.B. Hooper, J. Biol. Chem. 269 (1994) 11878–111871.

[107] J.A. Zahn, D.M. Arciero, A.B. Hooper, J.R. Coats, A.A. DiSpirito, Arch. Microbiol. 168 (1997) 362–372.

[108] J. Villalain, I. Moura, M.C. Liu, W.J. Payne, J. LeGall, A.V. Xavier, J.J. Moura, Eur. J. Biochem. 141 (1984) 305–312.

[109] C.G. Timoteo, P. Tavares, C.F. Goodhew, L.C. Duarte, K. Jumel, F.M. Girio, S. Harding, G.W. Pettigrew, I. Moura, J. Biol. Inorg. Chem. 8 (2003) 29–37.

[110] C.S. Nobrega, M. Raposo, G. Van Driessche, B. Devreese, S.R. Pauleta, J. Inorg. Biochem. 171 (2017) 108–119.

[111] M. Hoffmann, J. Seidel, O. Einsle, J. Mol. Biol. 393 (2009) 951–965.

[112] G.S. Pulcu, K.E. Frato, R. Gupta, H.R. Hsu, G.A. Levine, M.P. Hendrich, S.J. Elliott, Biochemistry 51 (2012) 974–985.

[113] R. Gilmour, C.F. Goodhew, G.W. Pettigrew, S. Prazeres, I. Moura, J.J. Moura, Biochem. J. 294 (Pt 3) (1993) 745–752.

[114] M. Ronnberg, T. Araiso, N. Ellfolk, H.B. Dunford, J. Biol. Chem. 256 (1981) 2471–2474.

[115] G.W. Pettigrew, S. Prazeres, C. Costa, N. Palma, L. Krippahl, I. Moura, J.J. Moura, J. Biol. Chem. 274 (1999) 11383–11389.

[116] N. Ellfolk, M. Ronnberg, R. Aasa, L.E. Andreasson, T. Vanngard, Biochim. Biophys. Acta 743 (1983) 23–30.

[117] S.J. Elliott, A.L. Bradley, D.M. Arciero, A.B. Hooper, J. Inorg. Biochem. 101 (2007) 173–179.

[118] C.F. Becker, N.J. Watmough, S.J. Elliott, Biochemistry 48 (2009) 87–95.

[119] N. Ellfolk, M. Ronnberg, R. Aasa, L.E. Andreasson, T. Vanngard, Biochim. Biophys. Acta 784 (1984) 62–67.

[120] A. Echalier, T. Brittain, J. Wright, S. Boycheva, G.B. Mortuza, V. Fulop, N.J. Watmough, Biochemistry 47 (2008) 1947–1956.

[121] N. Foote, J. Peterson, P.M. Gadsby, C. Greenwood, A.J. Thomson, Biochem. J. 223 (1984) 369–378.

[122] S. Prazeres, J.J. Moura, I. Moura, R. Gilmour, C.F. Goodhew, G.W. Pettigrew, N. Ravi, B.H. Huynh, J. Biol. Chem. 270 (1995) 24264–24269.

[123] M. Rönnberg, K. Osterlund, N. Ellfolk, Biochim. Biophys. Acta 626 (1980) 23–30.

[124] S.R. Pauleta, Y. Lu, C.F. Goodhew, I. Moura, G.W. Pettigrew, J.A. Shelnutt, Biochemistry 40 (2001) 6570–6579.

[125] S.R. Pauleta, Y. Lu, C.F. Goodhew, I. Moura, G.W. Pettigrew, J.A. Shelnutt, Biochemistry 47 (2008) 5841–5850.

[126] M.W. Wolf, K. Rizzolo, S.J. Elliott, N. Lehnert, Biochemistry 57 (2018) 6416–6433.

[127] S. Prazeres, I. Moura, J.J.G. Moura, R. Gilmour, C.F. Goodhew, G.W. Pettigrew, Magn. Reson. Chem. 31 (1993) 68–72.

[128] L. De Smet, G.W. Pettigrew, J.J. Van Beeumen, Eur. J. Biochem. 268 (2001) 6559–6568.

[129] R. Weiss, A. Gold, J. Terner, Chem. Rev. 106 (2006) 2550–2579.

[130] N. Foote, J. Peterson, P.M. Gadsby, C. Greenwood, A.J. Thomson, Biochem. J. 230 (1985) 227–237.

[131] C. Greenwood, N. Foote, P.M.A. Gadsby, A.J. Thomson, Chem. Scr. 28 (1988) 79–89.

[132] V. Fülöp, N.J. Watmough, S.J. Ferguson, Adv. Inorg. Chem. 51 (2001) 163–204.

[133] G. Smulevich, B.D. Howes, E. Droghetti, RSC Metallobiology (2016) 61–98.

[134] C.S. Nobrega, B. Devreese, S.R. Pauleta, Biochim. Biophys. Acta 1859 (2018) 411–422.

[135] M.H. Emptage, A.V. Xavier, J.M. Wood, B.M. Alsaadi, G.R. Moore, R.C. Pitt, R.J. Williams, R.P. Ambler, R.G. Bartsch, Biochemistry 20 (1981) 58–64.

[136] N. Ellfolk, M. Rönnberg, R. Aasa, T. Vanngärd, J. Ångström, Biochim. Biophys. Acta 791 (1984) 9–14.

[137] R. Gilmour, S. Prazeres, D.F. McGinnity, C.F. Goodhew, J.J. Moura, I. Moura, G. W. Pettigrew, Eur. J. Biochem. 234 (1995) 878–886.

[138] R. Gilmour, C.F. Goodhew, G.W. Pettigrew, S. Prazeres, J.J. Moura, I. Moura, Biochem. J. 300 (Pt 3) (1994) 907–914.

[139] G.W. Pettigrew, C.F. Goodhew, A. Cooper, M. Nutley, K. Jumel, S.E. Harding, Biochemistry 42 (2003) 2046–2055.

[140] V. Fulop, C.J. Ridout, C. Greenwood, J. Hajdu, Structure 3 (1995) 1225–1233.

[141] A. Echalier, C.F. Goodhew, G.W. Pettigrew, V. Fulop, Structure 14 (2006) 107–117.

[142] H. Shimizu, D.J. Schuller, W.N. Lanzilotta, M. Sundaramoorthy, D.M. Arciero, A.B. Hooper, T.L. Poulos, Biochemistry 40 (2001) 13483–13490.

[143] J.M. Dias, T. Alves, C. Bonifacio, A.S. Pereira, J. Trincao, D. Bourgeois, I. Moura, M.J. Romao, Structure 12 (2004) 961–973.

[144] L. De Smet, S.N. Savvides, E. Van Horen, G. Pettigrew, J.J. Van Beeumen, J. Biol. Chem. 281 (2006) 4371–4379.

[145] K.E. Ellis, J. Seidel, O. Einsle, S.J. Elliott, Biochemistry 50 (2011) 4513–4520.

[146] M. Ronnberg, N. Ellfolk, Biochim. Biophys. Acta 504 (1978) 60–66.

[147] N. Foote, R. Turner, T. Brittain, C. Greenwood, Biochem. J. 283 (Pt 3) (1992) 839–843.

[148] M. Ronnberg, N. Ellfolk, H.B. Dunford, Acta Chem. Scand. B 38 (1984) 79–83.

[149] M. Ronnberg, A.M. Lambeir, N. Ellfolk, H.B. Dunford, Arch. Biochem. Biophys. 236 (1985) 714–719.

[150] J.E. Erman, L.B. Vitello, J.M. Mauro, J. Kraut, Biochemistry 28 (1989) 7992–7995.

[151] M. Ronnberg, T. Araiso, N. Ellfolk, H.B. Dunford, Arch. Biochem. Biophys. 207 (1981) 197–204.

[152] H.C. Hsiao, S. Boycheva, N.J. Watmough, T. Brittain, J. Inorg. Biochem. 101 (2007) 1133–1139.

[153] Y. Lee, S. Boycheva, T. Brittain, P.D. Boyd, Chembiochem 8 (2007) 1440–1446.

[154] A. Morimoto, M. Tanaka, S. Takahashi, K. Ishimori, H. Hori, I. Morishima, J. Biol. Chem. 273 (1998) 14753–14760.

[155] H.B. Gray, J.R. Winkler, PNAS 102 (2005) 3534–3539.

[156] H.B. Gray, J.R. Winkler, PNAS 112 (2015) 10920–10925.

[157] R.D. Teo, R. Wang, E.R. Smithwick, A. Migliore, M.J. Therien, D.N. Beratan, PNAS 116 (2019) 15811–15816.

[158] K.E. Frato, K.A. Walsh, S.J. Elliott, Biochemistry 55 (2016) 125–132.

[159] C.M. Casadei, A. Gumiero, C.L. Metcalfe, E.J. Murphy, J. Basran, M.G. Concilio, S.C. Teixeira, T.E. Schrader, A.J. Fielding, A. Ostermann, M.P. Blakeley, E.L. Raven, P.C. Moody, Science 345 (2014) 193–197.

[160] M. Sundaramoorthy, J. Terner, T.L. Poulos, Structure 3 (1995) 1367–1377.

[161] R.M. Almeida, S. Dell'Acqua, L. Krippahl, J.J. Moura, S.R. Pauleta, Molecules 21 (2016) 1037.

[162] P.M. de Sousa, S.R. Pauleta, M.L. Goncalves, G.W. Pettigrew, I. Moura, M.M. Dos Santos, J.J. Moura, J. Biol. Inorg. Chem. 12 (2007) 691–698.

[163] P.M. Paes de Sousa, S.R. Pauleta, D. Rodrigues, M.L. Simoes Goncalves, G.W. Pettigrew, I. Moura, J.J. Moura, M.M. Correia Dos Santos, J. Biol. Inorg. Chem. 13 (2008) 779–787.

[164] D.L. Cameron, J. Jakus, S.R. Pauleta, G.W. Pettigrew, A. Cooper, J. Phys. Chem. B 114 (2010) 16228–16235.

[165] S.R. Pauleta, A. Cooper, M. Nutley, N. Errington, S. Harding, F. Guerlesquin, C.F. Goodhew, I. Moura, J.J. Moura, G.W. Pettigrew, Biochemistry 43 (2004) 14566–14576.

[166] G.W. Pettigrew, S.R. Pauleta, C.F. Goodhew, A. Cooper, M. Nutley, K. Jumel, S.E. Harding, C. Costa, L. Krippahl, I. Moura, J. Moura, Biochemistry 42 (2003) (1981) 11968–111961.

[167] S.R. Pauleta, F. Guerlesquin, C.F. Goodhew, B. Devreese, J. Van Beeumen, A.S. Pereira, I. Moura, G.W. Pettigrew, Biochemistry 43 (2004) 11214–11225.

[168] C.S. Nobrega, S.R. Pauleta, FEBS Lett. 592 (2018) 1473–1483.

[169] M. Koh, T.E. Meyer, L. De Smet, J.J. Van Beeumen, M.A. Cusanovich, Arch. Biochem. Biophys. 410 (2003) 230–237.

[170] G.W. Pettigrew, R. Gilmour, C.F. Goodhew, D.J. Hunter, B. Devreese, J. Van Beeumen, C. Costa, S. Prazeres, L. Krippahl, P.N. Palma, I. Moura, J.J. Moura, Eur. J. Biochem. 258 (1998) 559–566.

[171] C.S. Nobrega, I.H. Saraiva, C. Carreira, B. Devreese, M. Matzapetakis, S.R. Pauleta, Biochim. Biophys. Acta 1857 (2016) 169–176.

[172] K. Brown, D. Nurizzo, S. Besson, W. Shepard, J. Moura, I. Moura, M. Tegoni, C. Cambillau, J. Mol. Biol. 289 (1999) 1017–1028.

[173] M. Mirdita, K. Schutze, Y. Moriwaki, L. Heo, S. Ovchinnikov, M. Steinegger, Nat. Methods 19 (2022) 679–+.

[174] J. Jumper, R. Evans, A. Pritzel, T. Green, M. Figurnov, O. Ronneberger, K. Tunyasuvunakool, R. Bates, A. Zidek, A. Potapenko, A. Bridgland, C. Meyer, S.A. A. Kohl, A.J. Ballard, A. Cowie, B. Romera-Paredes, S. Nikolov, R. Jain, J. Adler, T. Back, S. Petersen, D. Reiman, E. Clancy, M. Zielinski, M. Steinegger, M. Pacholska, T. Berghammer, S. Bodenstein, D. Silver, O. Vinyals, A.W. Senior, K. Kavukcuoglu, P. Kohli, D. Hassabis, Nature 596 (2021) 583–589.

[175] P.M. Paes de Sousa, S.R. Pauleta, M.L. Simoes Goncalves, G.W. Pettigrew, I. Moura, J.J. Moura, M.M. Correia dos Santos, J. Biol. Inorg. Chem. 16 (2011) 209–215.

[176] M. Ronnberg, N. Ellfolk, Acta Chem. Scand. B 29 (1975) 719–727.

[177] W. Hu, L. De Smet, G. Van Driessche, R.G. Bartsch, T.E. Meyer, M.A. Cusanovich, J. Van Beeumen, Eur. J. Biochem. 258 (1998) 29–36.